MTR 407

LIGHT ATTENUATION WITH RESPECT TO SEAGRASSES IN SARASOTA BAY, FLORIDA

Submitted to

Sarasota Bay National Estuary Program

Mote Marine Laboratory Technical Report Number 407

ACKNOWLEDGEMENTS

The Principal Investigators thank the following for their assistance during this project: Kimberly Allen, Dan Dell'Armo, Patricia Minotti, Susan Murray, Kelly Naito, Ari Nissanka, and Jon Perry of Mote Marine Laboratory, and David Tomasko of the Sarasota Bay Project. Thanks also to Dr. Ernest Estevez, Linda Franklin, Dr. Don Hayward, and Jay Sprinkel in the compilation and preparation of the final report.

TABLE OF CONTENTS

LIST OF FIGURES

LIST OF TABLES

EXECUTIVE SUMMARY

A study to determine the factors contributing to water column light attenuation was conducted at the deep edges of seven seagrass beds in Sarasota Bay. *In situ* and water quality data were collected biweekly and attenuation was remeasured under a variety of controlled conditions in the laboratory. Monthly determinations of epiphytic attenuation and spectral absorption were conducted. Water column attenuation was partitioned into the fractions contributed by the water itself, color, chlorophyll, and nonchlorophyll suspended matter, and empirical regression models developed for field and laboratory attenuation.

Seasonal patterns of water column attenuation reflected the composite effects of patterns of turbidity or solids, chlorophyll, and color. Attenuation coefficients were low during the winter when biological activity and freshwater inflow were low, except during storm events. Influences of various attenuators were not uniform over the study area.

Laboratory partitioning of attenuation and spectral absorption measurements both indicated that water column attenuation was primarily attributable to the absorption and scattering of photosynthetically available radiation (PAR) by non-chlorophyll suspended matter. Non-chlorophyll suspended matter accounted for approximately 60 to 70 percent of water column attenuation.

The annual averages of PAR remaining in the water column at the maximum depth extent of two species of seagrasses (*Thalassia* and *Halodule*) typically ranged between 35 percent and 46 percent, averaging 42 percent. Light levels at one station were underestimated by sampling when solar angles were relatively low and recorded an annual average of 23 percent. Epiphytic attenuation averaged 50 percent for the study as a whole. Epiphytic attenuation was much higher in the winter when blade turnover was low.

Levels of PAR available to the seagrass blade were computed from time-adjusted K_d and epiphytic attenuation and averaged 21 percent on an annual basis with all stations combined. The levels of PAR available to the plant cannot be used as management goals for water column clarity unless epiphytic attenuation is zero.

Halodule was apparently able to tolerate extremely low levels of PAR during the winter, often below 10 percent. Both species, however, received an average of near 20 percent of incident (subsurface) PAR (after **combined** attenuation of water column and epiphytes) during the growing season (May through September). Comparison of total attenuation and with seagrass depth limits produced significant regressions, even with all station data.

The use of empirical regression models for the direction of management efforts should be performed with caution, as the regressions are not necessarily functional relationships. More weight should be placed on the partitioned results, in that they reflect

measurements of partitioned components, and are supported by the results of the spectral absorption work.

The interrelationships of epiphytic coverage with nutrient levels and water column clarity should be considered before water column targets are established in terms of maximum depth limits for seagrasses.

BACKGROUND

Seagrasses have been identified as keystone species which offer crucial habitat to numerous organisms within an estuary. The continued or improved health of seagrass beds is generally assumed to assist in the conservation and restoration of other desirable species. In addition to habitat value, the physical structure of grass beds can produce localized reductions in current regimes, thus providing an opportunity for water quality improvements through particulate settling.

Substantial losses of seagrasses have been identified in Tampa (Lewis, *et al.*, 1985) and Sarasota Bays, as well as in Charlotte Harbor (Harris *et al.*, 1983). As historical (non-catastrophic) losses of grasses throughout the Bay have been observed at the deeper edges of what were formerly extensive meadows, light limitation has been postulated as the major factor in the loss of cover. Reductions in light availability have been linked to seagrass declines throughout the world (Cambridge and McComb, 1984; Orth and Moore, 1983) and the Sarasota Bay Program has identified light availability as the primary abiotic factor controlling the coverage and robustness of the seagrass beds of Sarasota Bay. Increasing water clarity within the region remains one of the aims of the Sarasota Bay National Estuary Program.

From a resource management perspective, if increased light attenuation has reduced the extent of seagrass coverage by decreasing the effective depth to which the various species can penetrate, then an appropriate management goal is the direct or indirect control of light attenuating substances. Feasibility of control and the cost-benefits of control measures will depend in large measure upon which light attenuating substance (inorganic or detrital particles, phytoplankton, dissolved organics, or epiphytic material) accounts for the bulk of light reduction. Any selected control measures will also be forced to recognize typical seasonal fluctuations in runoff, color, chlorophyll concentrations, and overall water clarity.

Work in other regions on the components of light attenuation have identified very site-specific relationships for both the relative importance, and the consistency of effect, of the various water quality factors (Gallegos, *et al.*, 1991; Pierce, *et al.*, 1986; Gallegos, 1993). Color, chlorophyll, and suspended solids were the dominant contributors to attenuation in Tampa Bay and Charlotte Harbor (McPherson and Miller, 1987, 1994) but individual sites varied widely in their relative proportion of influence. Attenuating substances in Sarasota Bay were expected to vary similarly, reflecting a diversity of flushing rates, freshwater inflows, nutrient loading, and wave-induced resuspension experienced throughout the region.

RATIONALE

The partitioning of the components of light attenuation into an empirical model using standard water quality parameters such as color, chlorophyll, and the like, is not precise. While the full spectrum absorption due to chlorophyll pigments can be computed from literature values, visually-determined color measurements are less quantitative, and color exhibits spectral shifts not reflected in platinum-cobalt units. Scattering from particulate materials is not only wavelength dependent, but also is controlled by particle character and size, properties not measured by conventional suspended solids analyses.

Other difficulties for the construction of a model of attenuation exist as well. The inherent optical properties of absorption and scattering are caused by water, dissolved and particulate organic material, living pigmented particles (phytoplankton) and inorganic particles. The inherent optical property of the water column can be determined by the sum of the contributions of the individual components (absorption due to chlorophyll, to color, etc.). The vertical attenuation coefficient (K_d), however, is an "apparent" optical property of water (Preisendorfer, 1961; Kirk, 1983) and is dependent not only on the partial absorption and scatter ("inherent" optical properties), but also the angular and spectral distribution of the incident light. Any change in the overall absorption or scattering properties of the medium (through increasing one of the other components) will alter the absorption and scattering response of the other components. Accordingly, while an increase in component concentration is expected to increase vertical attenuation, the response will not likely be linear except within a narrow concentration range (Kirk, 1983), and the apparent optical property of attenuation is not truly additive from the attenuations measured or deduced from inherent attenuation components alone.

The dependence of K_d upon the character of the incident light field is related to whether the light field is collimated or diffuse. The light field near the surface is less diffuse on clear days, and therefore K_d values measured *in situ* may be lower near the surface on clear days than on cloudy days if all other factors are equal, even in well-mixed water. With increasing depth, the light field becomes more diffuse from particulate scattering, and variations become less discernible. Near-surface attenuation coefficients are, therefore, expected to vary substantially with differing solar conditions (time of day, direct sun, or hazy conditions).

As a result, as pointed out by Gallegos *et al.* (1991), partitioning the vertical attenuation coefficient, although widely used, is, at best, an approximation of the influence each attenuation component has on the total vertical attenuation coefficient, especially in turbid coastal water. Consequently, the value of K_d typically has a great deal of variability with respect to the partitioned components.

The project, therefore, was to measure not only *in situ* K_d, but also measured K_d in the laboratory under controlled lighting conditions. By using both a collimated light field, as well as a diffuse incident irradiance, the laboratory determined K_d should bracket the potential range of effects *in situ* due to differing character of surface illumination.

Laboratory attenuation was then to be partitioned into the components attributable to water, phytoplankton, dissolved substances (color), and, by difference, the attenuation attributable to non-chlorophyll suspended matter using the equations of Lorenzen (1972), as modified by McPherson and Miller (1987).

The removal of the variation attributable to incident light fields was expected to improve the significance of the correlations of laboratory K_d with partitioned attenuation coefficients and with measured water quality variables. Field measurements were also designed to collect information on both inherent and apparent optical properties, thus permitting an assessment of the relative influence of absorption and scattering on K_d.

The above procedures were designed to determine full spectrum (400-700 nm) water column attenuation, and relative importance of attenuating substances. Equivalent photosynthetically available radiation (PAR) levels, however, that differ in wavelength distribution (one predominantly green versus one stronger in the red and blue) will have different photosynthetic potential for seagrasses. The absorption spectrum of seagrass photosynthetic pigments has maxima in the blue and red ends of the visible light spectrum and a minimum in the green (Odum, 1985). Light absorption in the overlying water column is also wavelength dependent, with a minimum in the blue-green to green wavelengths, and red light much more rapidly attenuated than the shorter blue wavelengths. The four components that contribute to water column light absorption (water, dissolved color, phytoplankton, and suspended particulates [both inorganic and detrital]) each have a different spectral absorption profile (Roesler *et al.*, 1989).

Partitioning a total absorption spectrum (as might be measured on a raw, unfiltered sample) into the individual absorption spectra of dissolved color (gelbstoff), phytoplankton pigments and detritus (Kishino *et al.*, 1985; Roesler *et al.*, 1989), using spectrophotometer techniques, will evaluate how the distribution of light absorbing components affects the spectrum of light that reaches the seagrasses. The relative importance of various attenuators to the seagrass action spectra are expected to differ from the relative importance of those attenuators to the full PAR spectra.

In addition to water column attenuation, epiphytic loads on seagrasses are extremely relevant for any management actions which target light levels for the benefit of seagrasses. Dissolved and particulate water column materials may combine to produce an acceptable light climate for seagrass survival, but if nutrient concentrations support epiphytic loads which reduce the available light substantially, then seagrass survival may be jeopardized. Estimates of the further attenuation due to epiphytic material were to be provided roughly monthly, throughout the study year.

PROJECT SCOPE

The purpose of this project was to gather site- and seasonally-specific information on water column light attenuation components within Sarasota Bay. Vertical light

attenuation *in situ* was to be compared to laboratory generated values. Attenuation was also to be partitioned in the laboratory into that attributable to water, chlorophyll, dissolved organic matter (color), and non-chlorophyll suspended matter (NCSM) through the analysis of water quality parameters, and the measurement of the attenuation of both unfiltered and filtered samples.

Regressions of water quality parameters with measured attenuation were to be used to determine if consistent relationships existed for the Sarasota Bay area, to estimate the relative importance of attenuating factors, and more importantly, whether numeric water quality improvement goals could be reasonably and confidently established based on some desired water clarity. Limited investigations of spectral components of attenuation, and the attenuation attributable to epiphytic cover on seagrass blades, were also to be performed to estimate the total attenuation effected by both water column and epiphytic material at the various sites.

Funded in its entirety by the Sarasota Bay National Estuary Program, the project was accomplished as a cooperative venture between the Program Office and MML, with Program staff performing all field sampling, and MML performing laboratory analyses and the majority of the data reduction and report preparation. The project was designed with biweekly samplings of seven sites for *in situ* attenuation, with water samples collected for the laboratory analyses of color, chlorophyll 'a', total, volatile, and mineral suspended solids, turbidity, and specific conductance (and salinity). Laboratory attenuation coefficients were also determined on both unfiltered and filtered samples, using both collimated and diffuse light sources. On an approximately monthly basis, seagrass samples from the deep edges at the seven sites were collected for the determination of epiphytic attenuation, and water samples were processed for spectral absorption determinations.

METHODS

All field and laboratory activities were conducted under a U.S. Environmental Protection Agency-approved Project Quality Assurance Plan.

Sampling Locations

Stations were selected by the Program Office (Figure 1) to represent a variety of influences thought to be significant for the Bay, and also to represent a variety of seagrass health and productivity conditions (Tomasko *et al.*, in review). Locations ranged the length of the Sarasota Bay study area and are listed in Table 1, together with the depths to which seagrasses were observed. Access to stations was obtained via docks or bridges.

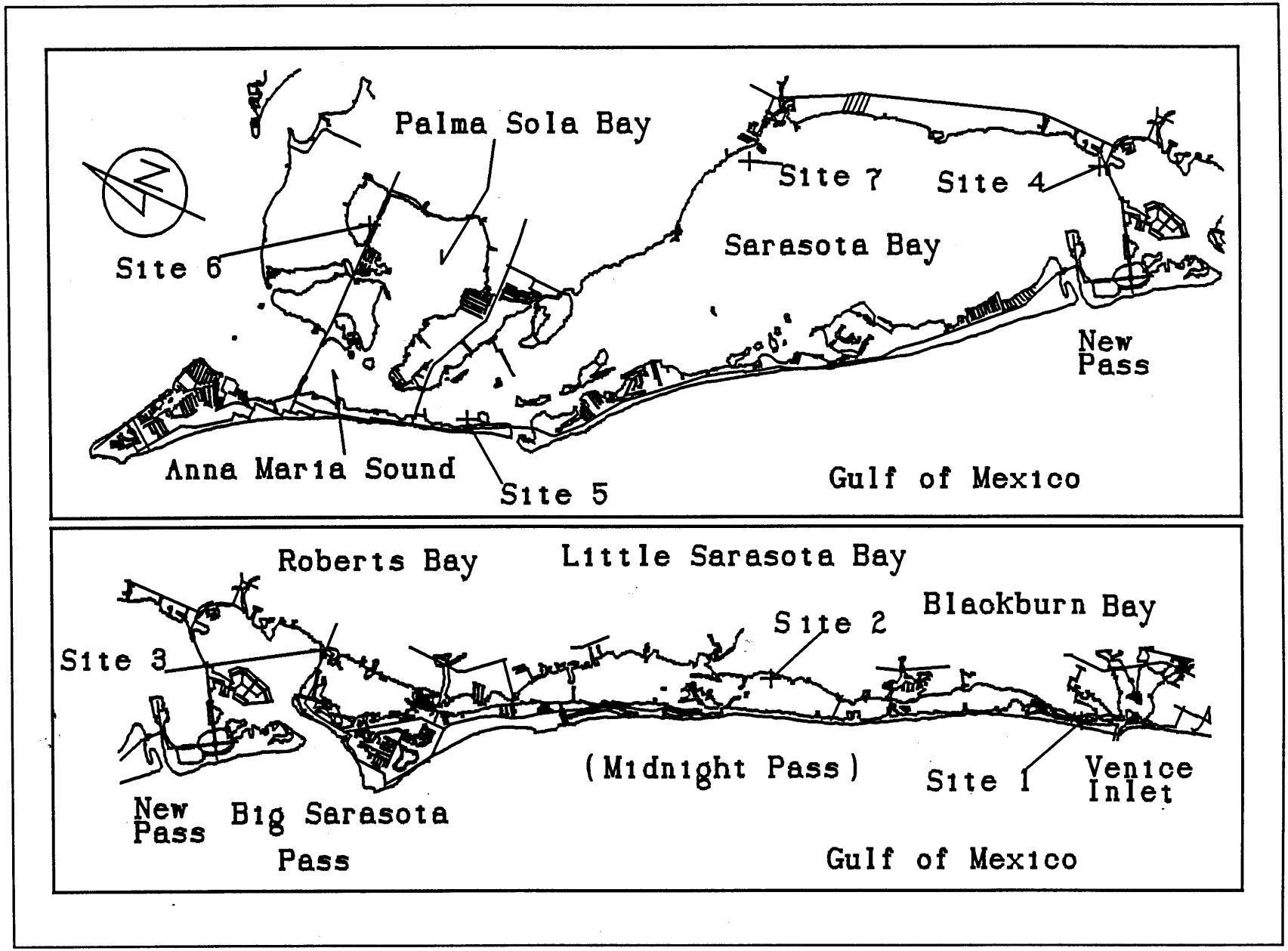

Figure 1. Station locations for water column and epiphytic material light attenuation. Sarasota Bay, Florida.

Table 1. Seagrass species present and maximum depths at Sarasota light attenuation stations.

Site	Designation	Species	Depth Extent (m below msl)
1	Blackburn Bay	*Halodule*	1.63
2	Little Sarasota Bay	*Halodule*	0.58
3	Roberts Bay	*Thalassia*	0.79
4	Ringling Causeway	*Halodule*	0.99
5	Anna Maria Sound	*Thalassia*	1.33
6	Palma Sola Bay	*Thalassia*	0.77
7	Cedar Hammock Creek	*Halodule*	0.50*

* - Grasses disappeared from immediate station location soon after study initiation. Extreme low tides and winter desiccation thought responsible.

Blackburn Bay (Site 1) is near the Venice Inlet, one of the connections of the Gulf of Mexico with the lagoonal Sarasota Bay system. Under high rainfall and freshwater discharge conditions, waters from the major drainage system of Cow Pen Slough and the Myakka River (via Curry Creek) can extend into this region of the study area. Seagrasses extended deeper at this location than at any other site. Tidal currents are notable on occasion. The Little Sarasota Bay site (Site 2) is in a region of the study area with comparatively low tidal flushing action, with numerous small tributaries, and relatively high freshwater inflows. Roberts Bay (Site 3) receives freshwater from the large Phillippi Creek drainage system, but also experiences tidal flushing as a result of proximity to Big Sarasota Pass and the Gulf of Mexico. All three of the Bays are very shallow (<6' in depth) water bodies. Although they consist of a relatively small portion of the surface area of the entire Sarasota Bay system, the three bays receive a large portion of the total nutrient loadings. The Intracoastal Waterway, with controlling depths of 9', runs the length of these three interconnected Bays.

The Ringling Causeway site (Site 4), is located in Sarasota Bay proper, between Big Sarasota and New Passes, and thus experiences comparatively greater tidal flushing. The location is relatively exposed to wind and wave action, and near the downtown region, is potentially influenced by urban stormwater. Sarasota Bay is deeper overall than the Blackburn, Little Sarasota, or Roberts Bays, with approximately two-thirds of the surface area at depths greater than 6', and maximum depths of 12'.

The Anna Maria Sound site (Site 5) is located quite near Longboat Pass and the Gulf of Mexico. The northern portion of the study area retains the most extensive and most productive seagrass beds in the region, and except for tidal swash channels and the Intracoastal Waterway, most of the immediate area is less than 6' in depth. The lower portion of Palma Sola Bay (most less than 6' in depth) has extensive seagrass beds, but 1988 photography showed coverage patterns indicative of retreating grassbeds in the area.

Site 6 in Palma Sola Bay has narrow fringing grassbeds along a causeway subject to intense recreational use.

The final station, at the mouth of Cedar Hammock Creek (Site 7), at the north end of Sarasota Bay, is in a region with undoubted urban stormwater influences and is exposed to southerly wind and wave action. The deep edges of the grasses at this site were the shallowest of all stations. Grasses disappeared from the Site 7 location shortly after the initiation of the study. A severe weather system, with a long period of high northerly winds and near freezing temperatures, produced extremely low tides during late October, 1994, and probably exposed the grassbeds at this location to desiccation.

In Situ Procedures

Field work consisted of biweekly efforts at seven selected stations over a calendar year for a total of 26 samplings. Samplings began October 27, 1993, and were completed October 19, 1994. Activities in the field consisted of the water column measurements of irradiance using integrating photosynthetically available radiation (PAR 400-700 nm) sensors. Upwelling and downwelling irradiance (E_u and E_d) were measured with cosine sensors (LI-COR 192SB), and scalar irradiance (E_o) with spherical or scalar sensors (LI-COR 193SA).

The three submersible sensors were attached to a lowering frame with depths marked in 0.2 m increments. Incident irradiance was simultaneously recorded with a cosine sensor in air (LI-COR 190SB) for later proportional corrections for changing incident conditions. Readings were collected as depth profiles at 0.2 meter increments, with the number of depths dependent on the water depth of the station at the time. During each sampling, two discrete depth profiles were recorded at each station. Measurements were made from structures (bridges, docks, etc.) with care taken to prevent shadowing of the light sensors by the structure. All light measurements were made as close to midday (solar noon) as possible (generally between the hours of 1000 and 1400, local time), and recorded on a common data logger. Time, sky condition, estimates of cloud cover, and other meteorological variables were recorded for each sample site.

During each biweekly sampling, surface grab samples were collected for later laboratory determinations of light attenuating substances, for a total of 181 samples. On an approximately monthly basis, five samples of entire shoots of seagrasses were collected from the deep edge of the grass bed at each station and attenuation from epiphytic cover on the seagrass blades was determined in the laboratory. Surface water samples collected during the biweekly samplings were also processed monthly for the spectral absorption of both dissolved and particulate materials. Eleven epiphytic coverage samplings (330 samples) and 12 spectral absorption samplings (84) samples were conducted.

Data Reduction of Field Measurements

Data reduction of field measurements included calculation of the vertical diffuse attenuation coefficient (K_d) between individual depths as:

$$K_d\,(z_1,z_2) = \frac{-\ln\left(E_d(z_2)/E_d(z_1)\right)}{z_2 - z_1}$$

where E_d is the downwelling irradiance as measured by the cosine sensor at depths z_1 and z_2. The incident irradiance readings (in air) were used to normalize $E_d(z_1)$ and $E_d(z_2)$ for changing atmospheric conditions. Additionally, water column K_d values were computed as the slope of the regression of the natural log of the downwelling irradiance [$E_d(z)$] against measurement depths, ignoring the slight non-linearity produced by differential absorption of various wavelengths. Replicate profiles were calculated separately and analyzed for variation. All profiles with negative values of K_d at individual depths or large discrepancies between replicate profiles were examined for outlier or spurious data and a total of 16 of 1147 data points were discarded. For regression analyses, replicate water column K_d values (determined through linear regression) were averaged provided that the correlation coefficient equaled or exceeded 0.8 ($n \approx 6$, or less) and that K_d was a positive value. *In situ* profiles were available for 178 station-date combinations.

Although not pertinent to the planned modeling of light attenuation, scalar "attenuation coefficients" were also computed similar to K_d above, due to the prevalence of this measurement in more biologically oriented monitoring programs. The scalar irradiance is indeed a more biologically relevant quantity, integrating the entire light field available to a macrophyte at a particular depth. The use of scalar measurements of irradiance for calculation of attenuation, however, either assume that upwelling light is inconsequential, or that scattering is minimal. In shallow turbid areas of the study area, with a high potential for bottom reflectance, these assumptions may not hold universally. As a result, $K_{d\,scalar}$ was computed to present a comparison with K_d for the potential extension of these results to other monitoring programs, but was not modelled extensively.

Downwelling irradiance, upwelling irradiance, and scalar irradiance were used to compute the average cosine of photon zenith angles for total light [$\bar{\mu}(z)$ - scattering dependent], the vertical attenuation coefficient for net downward irradiance [$K_E(z)$] and the absorption coefficient [$a(z)$] (Kirk, 1992). These parameters provide an empirical means to compare the relative importance of scattering and absorbing material between sites, independent of water quality parameters, and were calculated as follows, again normalizing for changing incident conditions based on measurements in air:

$$\bar{\mu}(z) = \frac{E_d(z) - E_u(z)}{E_o(z)}$$

$$K_E(z) = \frac{-\ln\left((E_d(z_2) - E_u(z_2))/(E_d(z_1) - E_u(z_1))\right)}{z_2 - z_1}$$

$$a(z) = K_E(z) \bullet \bar{\mu}(z)$$

For regression analyses, $\bar{\mu}$ and a were calculated as the arithmetic average of all values obtained at a station, while K_E was computed as an average of the slopes of the linear regression of the natural log of the difference between downwelling and upwelling irradiance, as a function of depth between replicate profiles.

Adjusted Attenuation Coefficients

While samplings were conducted between the hours of 1000 and 1400 (local time) on all days in which water column measurements were obtained, sites were always visited in the same order. Average solar elevation of all measurements made at the individual sites, therefore, ranged from 44.5° to 62.4° (Figure 2) with solar elevations during Site 1 measurements an average of 17° lower than local noon. Elevations at local noon ranged from 38° to 85° throughout the sampling year.

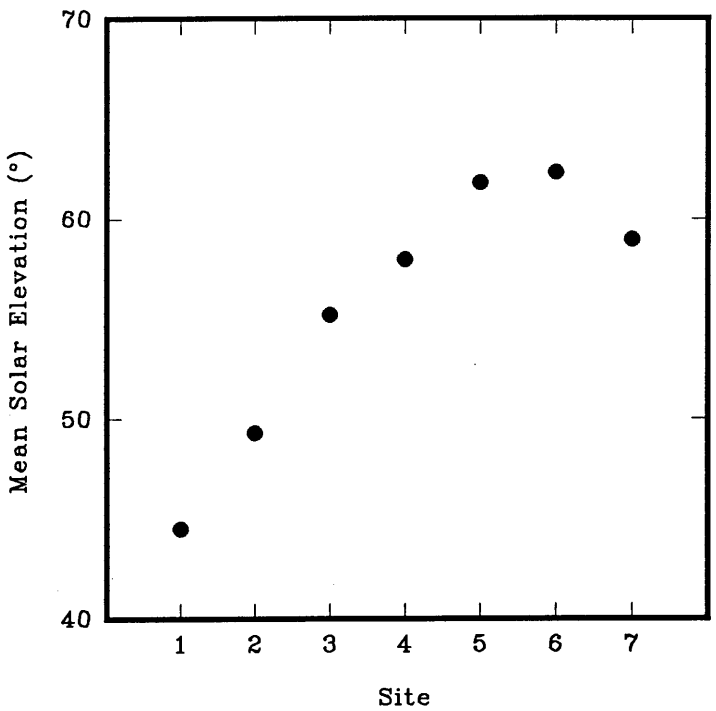

Figure 2. Mean solar elevations by station during *in situ* measurements.

To allow for station intercomparisons and to account for the longer effective path length required to reach a sensor at specific depth when solar elevations are lower, solar elevations were calculated from time (EST) and date, using a latitude of 27°20' (Kirk, 1983). Solar zenith angle (Θ_a) and the refractive index of water were used to compute the cosine of the zenith angle in water (Θ_w) to correct K_d measurements to $K_{d\ adj}$ (Figure 3) by:

$$K_d(O,z) = \frac{-\ln\left(E(z) - E(O)\right)}{z}$$

$$K_{d\ adj} = \frac{-\ln\left(E_d(z) - E_d(O)\right)}{z_{adj}}$$

$$= \frac{-\ln\left(E_d(z) - E_d(O)\right)}{z} \bullet \frac{z}{z_{adj}}$$

$$= K_d \bullet \mathrm{Cos}\ (\Theta_w)$$

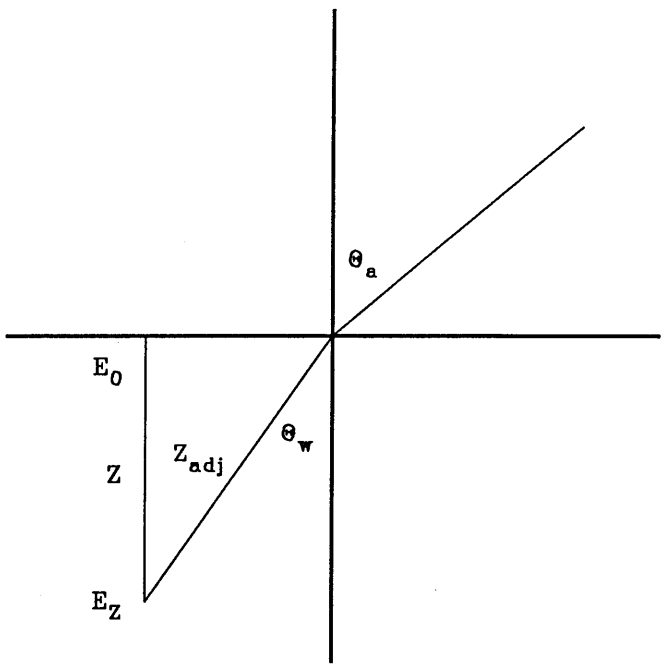

Figure 3. Geometry for calculation of $K_{d\ adj}$ for low solar elevation analyses (B).

The approximate correction for low solar elevations, while used to compare stations sampled at differing times of day, and to determine the relationship of water quality parameters with diffuse attenuation, does not reflect absolute *in situ* light environments. The correction endeavors to calculate the attenuation coefficient as if the sun were directly overhead ($\Theta_a = 0°$), even during the winter months when maximum daily solar elevations reach only 40°($\Theta_a = 50°$). Additionally, the correction ignores scattering effects, and so the efficacy of the correction is expected to be lower for measurements with large scattering components and diffuse light conditions.

Laboratory Procedures

Laboratory parameters and references used in the project appear in Table 2. Conventional water quality parameters all use EPA-approved methodologies. Methods with no EPA-approved equivalent include those for the determination of diffuse and collimated attenuation coefficients, spectral absorption of the suspended and dissolved components, and the light attenuation attributable to epiphytic material, described below.

Table 2. Laboratory methodologies for water quality parameters.

Parameter	Method	Description
Color	2120B[1]	Visual, nessler tube
Chlorophyll 'a'	10200H[1]	Acidification and trichromatic
Total Suspended Solids	2540D[1]	Gravimetric
Volatile Suspended Solids	2540E[1]	Gravimetric
Mineral Suspended Solids	by calculation[1]	
Turbidity	2130B[1]	Nephelometric
Specific Conductance	120.1[2]	Electrical resistivity
Salinity	by calculation[3]	

1 Standard Methods for the Examination of Water and Wastewater, APHA, AWWA, WPCF, 17th Edition

2 Methods for the Chemical Analysis of Water and Wastes, EPA-600/4-79-020, 1979, Revised March 1983.

3 Jaeger, 1973

Laboratory Attenuation Coefficients

The laboratory determinations of K_d were determined in a manner similar to McPherson and Miller (1987), but with several modifications developed at MML.

Laboratory attenuation measurements on both unfiltered (raw) and filtered samples were made with both collimated and diffuse irradiance sources. Collimated light was used to

determine $K_{dCOL-RAW}$ and $K_{dCOL-FILT}$, representing near-surface measurements on a clear day. A frosted glass diffuser was then placed in the light path and attenuation measurements repeated to obtain $K_{dDIF-RAW}$ and $K_{dDIF-FILT}$, measurements more representative of sub-surface attenuations on a cloudy day.

Attenuation was measured with the apparatus depicted in Figure 4. A light source (300 W, quartz-halogen projector lamp) was focussed and collimated through a pinhole aperture, and the beam aligned downward through the sample tube. The spectrum for this source was assumed to be equivalent to that depicted in LI-COR (1982). To obtain a diffuse light source, the frosted glass diffuser was inserted at the lower end of the collimating tube.

The sample was contained in a 110.0 cm long, 4.8 cm internal diameter polycarbonate tube, with a drain, filling funnel, pinch clamp, and cosine sensor (LI-COR 192SB) secured to the bottom. The outer diameter of the sensor was equivalent to the internal diameter of the sample tube, although the sensor face area represented only approximately 5 percent of the cross sectional area of the tube. The tube was lined both inside and out with metallized Mylar to improve the reflectivity of the tubing walls and to prevent the excessive loss of scattered light, particularly for samples high in particulates. The scattered light should be returned to the test water column to simulate measurements made *in situ* in which parcels of water adjacent to the test sample would provide a scattered component. The return of scattered light to the sample tube is appropriate for both the collimated and diffuse measurements. Other variables being equal, the laboratory K_d value obtained should be reduced relative to the McPherson and Miller (1987) technique.

Sensor response was verified on each day laboratory attenuation was determined with the use of a 10 percent neutral grey transmittance filter. The sample was introduced into the tube through the filling funnel and the water column heights inside the tube determined from using the filling funnel tubing as a sight glass. Filling the sample tube from the bottom allowed sample to be introduced without changing sample tube alignment. The sample tube could be filled rapidly, and yet without aeration, and irradiance measurements taken quickly before particulates could settle. The sample tube was rinsed with an aliquot of the sample and then irradiance measurements were made with the tube filled to approximately the 30.0 cm and 100.0 cm marks above the sensor face. (During the first sampling, 10.0 cm rather than 30.0 cm was used for the initial depth.) Blanks of deionized water were processed identically to all samples at the beginning and end of each day of analysis.

Calculation of the collimated and diffuse K_d values differed due to the imperfect optics of the collimating tube and the less than 100 percent reflection afforded by the mylar tube lining. The corrections and calculations for each type of K_d are described below.

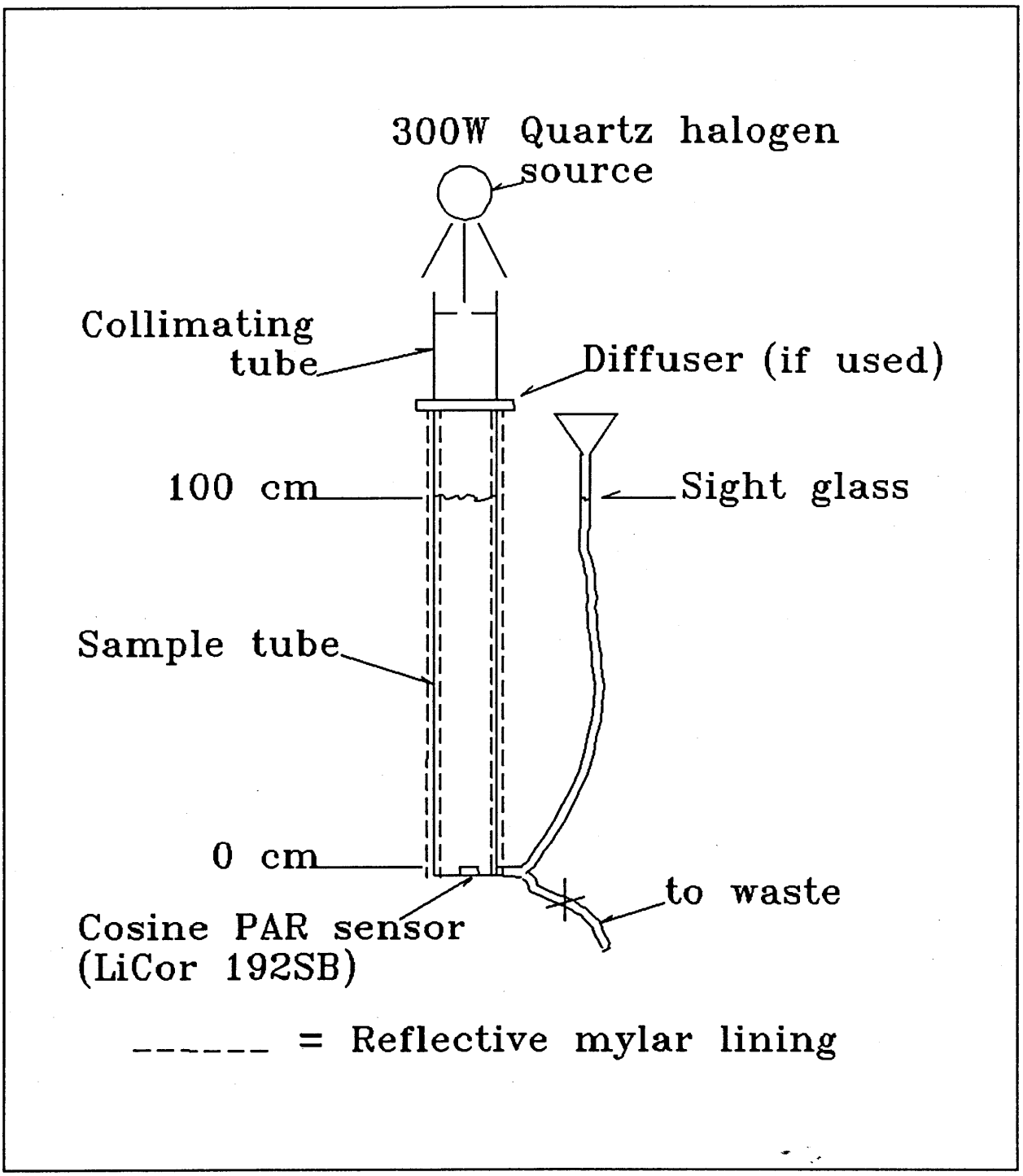

Figure 4. Apparatus for determination of laboratory PAR attenuation.

Diffuse Laboratory Attenuation Coefficient

For diffuse light, a series of tests demonstrated that irradiance (measured in air) decreased noticeably with distance from the source, indicating a scattering loss of diffuse light through the walls of the tube. (The light field in the horizontal plane was assumed to be uniform within the sample tube.) Irradiance at the surface of the water for the 30.0 cm measurement was approximately 30 percent lower than the irradiance at the surface of the 100.0 cm column of water. Additional losses of diffuse light were observed through the walls of the tube when in water.

A series of measurements in air, at different distances from the source, as well as a series of irradiance measurements of deionized water blanks at multiple depths with the sensor at a fixed distance were used to compute the **observed** attenuation coefficients of pure water at multiple depths. The integrated (400-700 nm) beam attenuation coefficient for pure water and a quartz-halogen spectrum (LI-COR, 1982) was also computed for each measurement depth. The attenuation coefficients observed in the apparatus were then reduced by twice the beam attenuation coefficient of pure water at the measurement depth, assuming that the optical path of diffuse light was twice that of a collimated beam of light (Butler, 1962), i.e., reduced by $2 \bullet 0.219$ m^{-1} for 100.0 cm of water. The attenuation coefficient remaining represented the scattering loss through the walls of the tube, plus the losses at the air-water interface, and the average correction factor was 0.319 m^{-1}.

During each analytical run, irradiance readings of blank (deionized) water at the 30.0 and 100.0 cm depths, the apparatus loss from scattering and reflection (0.319 m^{-1}), and twice the theoretical beam attenuation coefficient water for that depth ($2 \bullet 0.230$ m^{-1} for 0.3 m, $2 \bullet 0.219$ m^{-1} for 100.0 cm) were used to back-calculate the incident irradiance just above the surface of the water column for all 30.0 cm and 100.0 cm readings. The sample readings were subsequently proportionally adjusted to reflect the differing incident irradiance and an observed attenuation coefficient was calculated through the use of:

$$K_{dDIF} = \frac{- \ln \left(E_d(z_2) / E_d(z_1)\right)}{z_2 - z_1}$$

The observed attenuation coefficient so calculated, however, still included the "attenuation" attributed to the loss at the air/water interface and through the walls of the tube. Observed attenuation coefficients were accordingly reduced by the correction factor determined above, 0.319 m^{-1}, with the resultant $K_{dDIF\text{-}RAW}$ representing the attenuation produced by water, dissolved organic matter, and suspended particulates, and $K_{dDIF\text{-}FILT}$ representing the attenuation produced by water and dissolved organic matter alone.

Collimated Laboratory Attenuation Coefficient

For collimated light, irradiance measurements indicated that the slight degree of non-collimation of the source was rapidly magnified upon entry into the sample apparatus. The beam was apparently focussed by the tube, and since the sensor measured only 5 percent of the cross sectional area, total irradiance for a given measurement distance could not be determined. The measured irradiance was non-linear and **inversely** related to distance from the source, with a maximum reading when the sensor coincided with the tube's effective focal point. The distribution of the light field in the horizontal plane was assumed to be non-homogenous and so measurements at different depths were not comparable, although irradiance measurements of sample and blank at the same depths could be used to determine the attenuation attributable to sample components (dissolved organic matter, particulates).

Collimated laboratory attenuation coefficients were therefore calculated for each depth as:

$$K_{dCOL} = \frac{-\ln \left(E_d(z_1,\text{SAMPLE}) \ / \ E_d(z_1,\text{BLANK})\right)}{z_1}$$

The K_{dCOL} calculated above, however, no longer include the attenuation due to water alone, and so the values were further adjusted, adding back in the beam attenuation coefficient for water under a quartz-halogen spectrum, as appropriate for the specific z_1 (i.e., add 0.230 m^{-1} for 30.0 cm depth, 0.219 $^{-1}$ for 100.0 cm depth). The optical path was assumed to be 1.0 and equal for both blank and sample values, an assumption most appropriate for filtered samples. The optical path of samples high in particulates would undoubtedly be greater than 1.0 and the $K_{dCOL\text{-}RAW}$ calculated, by under representing attenuation due to water, may be an underestimate for raw samples high in particulates, especially for the 100.0 cm measurements. Similarly, the scattering in raw samples would be expected to have additional losses through the wall of the apparatus, conversely producing an overestimate of the "true" value of K_{dCOL}. Fortunately, the effect of increasing depth is not large, as K_{dCOL} for raw samples at 100.0 cm depths only averaged 0.05 m^{-1} lower than K_{dCOL} at 30.0 cm. The two values of K_{dCOL} computed for filtered samples agreed, on average, within 0.02 m^{-1}.

The low levels of irradiance and experimental precision resulted in several occasions when irradiance levels measured for samples were greater than the blank measurements, particularly for the 30.0 cm readings. Differences were within expected analytical precision of 2 $\mu E/cm^2$, however, averaging 0.7 $\mu E/cm^2$. In these instances, the K_{dCOL} computed from the 100.0 cm reading alone was used for regression analyses and partitioning of total water column attenuation.

Suspended and Dissolved Spectral Absorption

On a monthly schedule, the raw water sample from each station was filtered through a glass fiber filter (Whatman, GF/F) and the optical density (OD) spectrum (400 and 700 nm) of the particulate matter (detrital, mineral and chlorophyll) on the filter pad was measured relative to a blank, wetted filter in a scanning, dual-beam spectrophotometer (Varian, DMS-80). A blank baseline was measured with no filters in the light paths before and after each set of samples and the mean of these baselines was subtracted from all scans for that sample set. The calibration of the spectrophotometer was checked against calibration standards (Milton Roy) before and after running each set of samples.

After the OD spectrum was measured for the raw particulate matter, each filter containing the particulate was placed in methanol (Kishino *et al.*, 1985) for at least 50 minutes to extract the phytoplankton pigments. Following the methanol extraction the OD of the particulate (now only detrital and mineral) was measured again. These filter pad OD (OD_f) spectra were converted to suspension optical density (OD_s) spectra by correcting for pathlength amplification (ß; Butler, 1962) caused by multiple reflectance associated with the concentration of particles on the filters (Cleveland and Weidemann, 1993). The OD_s spectra were converted to absorption spectra using the following equation:

$$a_i(\lambda) = 2.3 \bullet (OD_{s,i}(\lambda)/pl)$$

where $a_i(\lambda)$ is the spectral absorption coefficient (m^{-1}) for each component (raw particulate and detrital) and pl is the pathlength equivalent to the volume of water filtered divided by the clearance area of the filter. Phytoplankton pigment absorption spectra (a_p) were obtained by subtracting the detrital absorption (a_d) spectra (after methanol extraction) from the raw particulate (a_{rp}) spectra (before methanol extraction).

The dissolved color absorption spectra were obtained using the water filtrates from the above filtrations. The optical density spectrum of this filtered water was measured against double distilled water in 10 cm cuvettes using the same spectrophotometer described above. The dissolved color optical density spectra were converted to absorption spectra (a_{dc}) using the above equation with OD_s replaced by the dissolved color optical density (OD_{dc}) and $pl = 0.1$ m.

The maximum, normalized, photosynthetically usable radiation spectrum ($PUR_{m\text{-}n}(\lambda)$) for seagrass at the maximum depth of seagrass growth at each station, based on absorption of water alone in the water column, was estimated using the following equation:

$$PUR_{m\text{-}n}(z,\lambda) = E(0,\lambda) \bullet e^{(-(a_w(\lambda))xz)} \bullet a_{sg\text{-}n}(\lambda)$$

where $E(0,\lambda)$ is spectral irradiance just below the water surface, $a_w(\lambda)$ is the spectral absorption coefficient of pure seawater, z is the depth (m) of the edge of the seagrass

bed, and $a_{sg\text{-}n}(\lambda)$ is the normalized spectral absorption coefficient of *Thalassia testudinum* (Odum, 1985). The normalized PUR for seagrass at the maximum depth of seagrass growth at each station, based on <u>total</u> absorption in the water column, was estimated as follows:

$$PUR_n(z,\lambda) = E(0,\lambda) \bullet e^{(-(a_w(\lambda) + a_{dc}(\lambda) + a_{tp}(\lambda))xz)} \bullet a_{sg\text{-}n}(\lambda)$$

The fraction of PUR(z) loss attributable to each of the absorbing components described above (dissolved color, pigments, and detritus) was calculated as follows:

$$FL_i(z) = \Sigma(PUR_{m\text{-}n}(z,\lambda) - PUR_n(z,\lambda)) \bullet a_i(\lambda) / a_t(\lambda)$$

where $a_t(\lambda) = a_{dc}(\lambda) + a_p(\lambda) + a_d(\lambda)$.

<u>Epiphytic and Total Attenuation</u>

For each sampling of epiphytic material, five samples of *Thalassia* or *Halodule* (one species/station) were collected from each station. Samples consisted of individual containers of one or more shoots, with the obviously necrotic portions (and associated epiphytic material) removed and discarded in the field. Laboratory processing consisted of the further dissection and discard of necrotic portions of the blades and gentle scraping of both epiphytes and epifauna (referred to collectively as epiphytes or epiphytic material) from both sides of the productive portions (non-necrotic blades above the blade-sheath boundary) of one or more shoots with razor blades. The structure of any epibiota (such as bryozoans) was retained as much as possible. Total blade area scraped (lengths • average width) was also determined.

To determine epiphytic attenuation, the suspension of scraped material was placed into a transparent (acrylic) dish. The area of the dish was selected based on the total surface area (2 • blade area) of a "typical" shoot, empirically determined at the beginning of the project. A dish of 71.3 cm^2 was used for *Thalassia* and 20.3 cm^2 for *Halodule*. Later in the study, as blade area per shoot varied, the number of shoots to scrape for each sample was increased to make the area scraped as close as possible to the dish area. Whenever more than one shoot was scraped, the entire additional shoot was processed, such that attenuation values are on a per shoot average basis.

PAR attenuation measurements were performed with the apparatus illustrated in Figure 5. The walls of the transparent dish were lined with reflective mylar, and the dish illuminated with a quartz-halogen light source (Dyna-Lume 240-350) and a white acrylic diffusing slide. A cosine PAR sensor (Locker 190SB) was placed 12 cm below the dish with epiphytes in the center of a column of the same size as the dish. The sensor tube was also lined with reflective mylar. For each sample, a blank reading of the irradiance passing through an equivalent depth of deionized water was determined, followed by three successive readings of the irradiance penetrating the epiphyte suspension. The

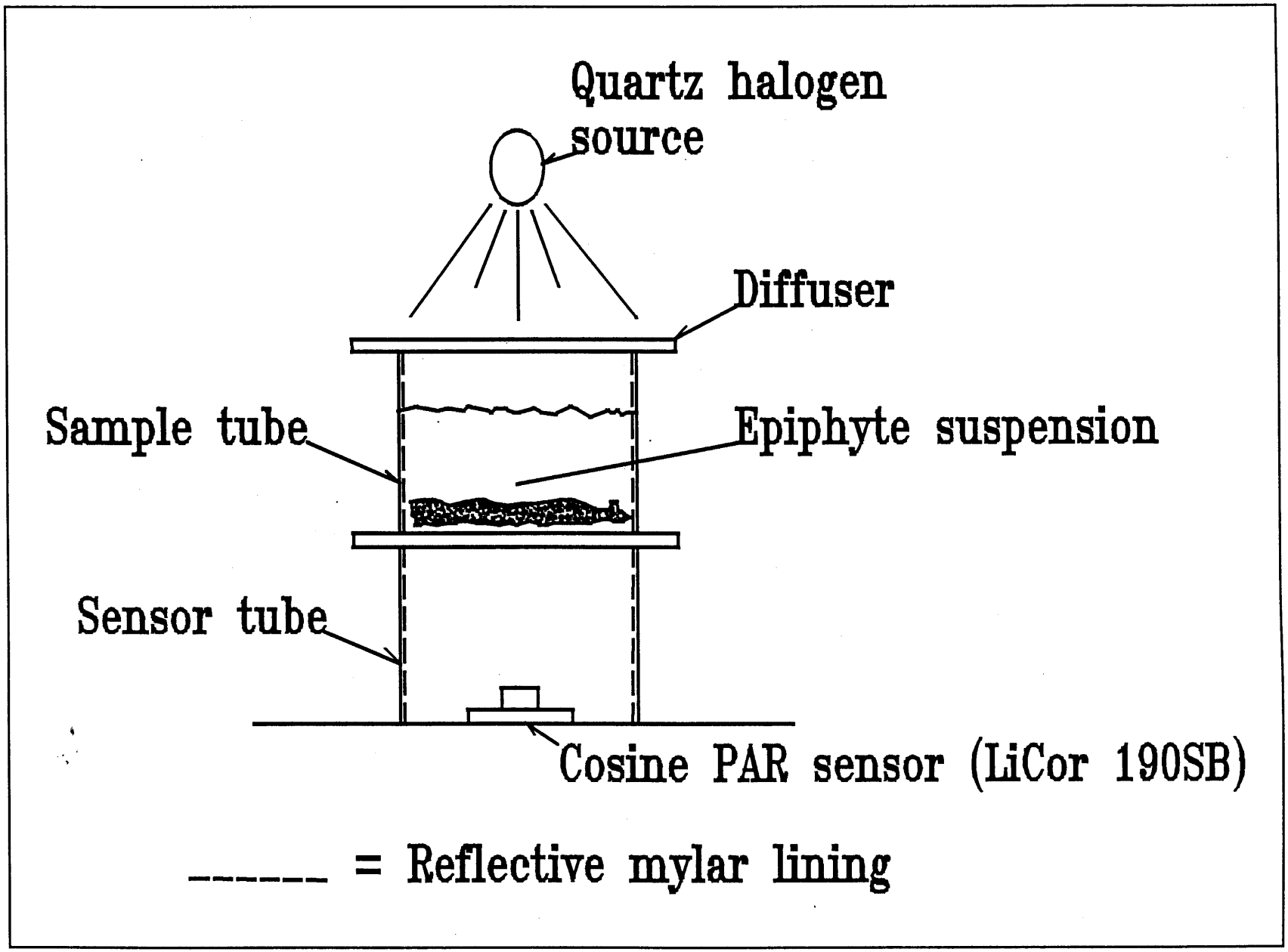

Figure 5. Apparatus for determination of PAR attenuation due to epiphytic material.

suspension was manually stirred and irradiance allowed to stabilize between each reading. Sample volumes (and therefore water depths) were held constant.

The inverse logarithmic relationship between the epiphyte suspension density and transmitted irradiance was used to correct for inequalities between dish area and blade area scraped. Analogous variables to epiphyte suspension density could also be blade area scraped (assuming a homogenous distribution of epiphytes over all leaf surfaces), or dish area in which a fixed amount of epiphytes were measured. The line established by the irradiance of the blank (dish area = 0) and the irradiance of the sample (dish area = 20.3 or 71.3 cm^2) was used to compute the irradiance which would have been measured had the dish area equalled the area scraped (i.e., epiphytic density in dish equivalent to average *in situ* conditions). The blank and corrected irradiance were then used to compute a corrected attenuation.

Seagrass Available PAR

The total light available to seagrasses is a combination of the amount transmitted by the water column **and** by the epiphytic load on the seagrass blades. To compute the annual and monthly light levels received by the plants, a 365 day period beginning October 27, 1993, was identified. *In situ* water column attenuation (cosine sensor) determined at a station on that day was adjusted for sun angle and extended to all subsequent days until the next sampling. The attenuation measured during the final sampling was extended until October 26, 1994. A similar extrapolation of sampled values was performed for the epiphytic attenuation, using the arithmetic mean of all five samples measured. Epiphytic attenuation for the period from October 27 until December 6, 1994 (the first determination of epiphytic attenuation) was set equal to that measured on December 6, 1993.

Daily values of the percent of available light **in the water column** at the deep edge (as a percent of incident light) were computed from the field attenuation coefficients and the maximum depths (Table 1). Tidal signals were assumed to cancel out and were not considered. The percentage of epiphytic attenuation was applied to the remaining water column light levels to generate daily values of the percent PAR available to the **seagrasses** during the midday hours. Daily values were averaged over month and year by station for comparisons. Percentages of light refer to a percentage of the irradiance just below the surface of the water. Values for October include days in both 1993 and 1994. It should be recalled that the $K_{d\ adj}$ used to compute water column light is a slight overestimate of *in situ* conditions, particularly during the winter months.

Partitioning of Attenuation Coefficient

Laboratory attenuation coefficients, both K_{dCOL} and K_{dDIF}, were partitioned analogous to the techniques in McPherson and Miller (1987). The attenuation due to suspended particulates ($K_{dCOL\text{-}PART}$ and $K_{dDIF\text{-}PART}$) was determined by difference between the raw

and filtered measurements. The beam attenuation coefficient due to pure water (100.0 cm path, tungsten-halogen spectra) and absorption coefficient due to chlorophyll were taken from literature values, 0.219 m^{-1} for water (LI-COR, 1982), and 0.0138 m^2/mg • uncorrected chlorophyll *a* mg/m^3 (Lorenzen, 1972). Lorenzen's values for chlorophyll *a* (determined trichromatically) were made for waters with much lower chlorophyll content, but were based on the integrated spectral attenuation of suspensions of phytoplankton in a spectrophotometer. The absorption coefficient is likely to be very appropriate for the work with the quartz-halogen source used in the present study. The attenuation due to non-chlorophyll suspended matter (NCSM) was computed as the particulates less that due to chlorophyll. Units are in m^{-1}, and final equations used were:

$$K_{dCOL\text{-}WATER} = 0.219$$

$$K_{dCOL\text{-}COLOR} = K_{dCOL\text{-}FILT} - K_{dCOL\text{-}WATER}$$

$$K_{dCOL\text{-}CHL} = 0.0138 \bullet \text{Chlorophyll } a \text{ (in } mg/m^3)$$

$$K_{dCOL\text{-}PART} = K_{dCOL\text{-}RAW} - K_{dCOL\text{-}FILT}$$

$$K_{dCOL\text{-}NCSM} = K_{dCOL\text{-}RAW} - K_{dCOL\text{-}FILT} - K_{dCOL\text{-}CHL}$$

For attenuation determined with diffuse light, similar equations were used with the exception that the beam attenuation values in the literature were multiplied by 2 to represent the increase in optical path length with diffuse light.

$$K_{dDIF\text{-}WATER} = 0.219 \bullet 2$$

$$K_{dDIF\text{-}CHL} = 0.0138 \bullet 2 \bullet \text{Chlorophyll a (in } mg/m^3)$$

By the calculations above, in the fully partitioned attenuation, $K_{d\ NCSM}$ also includes all error terms. In addition, with an increase in NCSM and scattering, an increase in optical path length occurs, thus increasing the potential for absorption. A portion of the "error" term contained within $K_{dCOL\text{-}NCSM}$, therefore, includes any additional absorption by chlorophyll, color, and water that results from optical path lengths greater than 1.0. Component attenuation values were also further reduced for presentation as a percentage of the total attenuation measured in the raw sample.

Correlation Analyses

The measured optical properties, both field and laboratory determined, were regressed against water quality parameters to ascertain which water quality parameters have significant correlation with inherent or apparent optical properties. Agreement between field and laboratory data were examined. Multiple linear regressions analyses were

conducted with NWA STATPAK 4.1 (1986), with critical values of F drawn from Sokal and Rohlf (1969).

RESULTS AND DISCUSSION

Water Quality Parameters

Variation in analytical water quality parameters (Table 3) was typically large, with percent relative standard deviation (%RSD) of most parameters exceeding 50 percent for the entire study. Salinity (or conductivity) was the only exception, with a 15 percent RSD, and salinity ranging from 10 to 34 ppt. Variations within a given station were also comparably large for all parameters except salinity. Seasonal patterns predominated, with high color values accompanying the onset of the wet season from August through the latter months of the study (Figure 6). Maximum values of color were 120 PCU, and Site 1, followed by Sites 2 and 3 recorded the most incidences of color greater than 50 PCU, while Site 7 recorded the highest average color values. Salinity data in general mirrored color distribution with the lowest salinities observed at Sites 7 and 1.

Chlorophyll *a* concentrations were typically below 30 mg/m^2, but larger values up to 100.7 mg/m^2 were recorded at Sites 7, 6, and 2. Chlorophyll data also were highly variable, but peak values generally were observed in late summer and fall (Figure 6).

Suspended solids and turbidity were high on occasion during March and April and appear most closely linked with storm events in 1994 (Figure 6). While turbidity was generally less than 10.0 NTU and suspended solids less than 30.0 mg/l, Sites 4 and 2 recorded the most extreme events for these parameters, up to 38.0 NTU and 60.1 mg/l. Volatile suspended solids (VSS) comprised between 20 percent and 60 percent of total suspended solids with the larger percentages appearing during June and July, and during the latter portion of the wet season. Higher VSS percentages during the summer and wet season presumably reflect both the chlorophyll component of suspended solids, and the detrital portions accompanying freshwater inflows.

In Situ Diffuse Attenuation Coefficients

In situ water column attenuation was quite variable, with attenuation coefficients (cosine sensor) observed as high as 4.04 m^{-1}. Almost all values (98%), however, were below 3.00 m^{-1}, and the average of all attenuation coefficients recorded for the study was 1.24 $\pm$ 0.59 m^{-1}. Repeated measurements at a station typically agreed well, with the standard deviation of replicate profiles in the field averaging 0.16 m^{-1}. From the average attenuation coefficients by station, Site 5 (Anna Maria Sound) experienced the clearest water conditions (0.83 m^{-1}) and Site 7 the least (1.82 m^{-1}). Extreme attenuation values accompanied one of the extremes of turbidity, color, or chlorophyll and seasonal patterns in K_d were a composite of the seasonal patterns of water quality parameters (Figure 6).

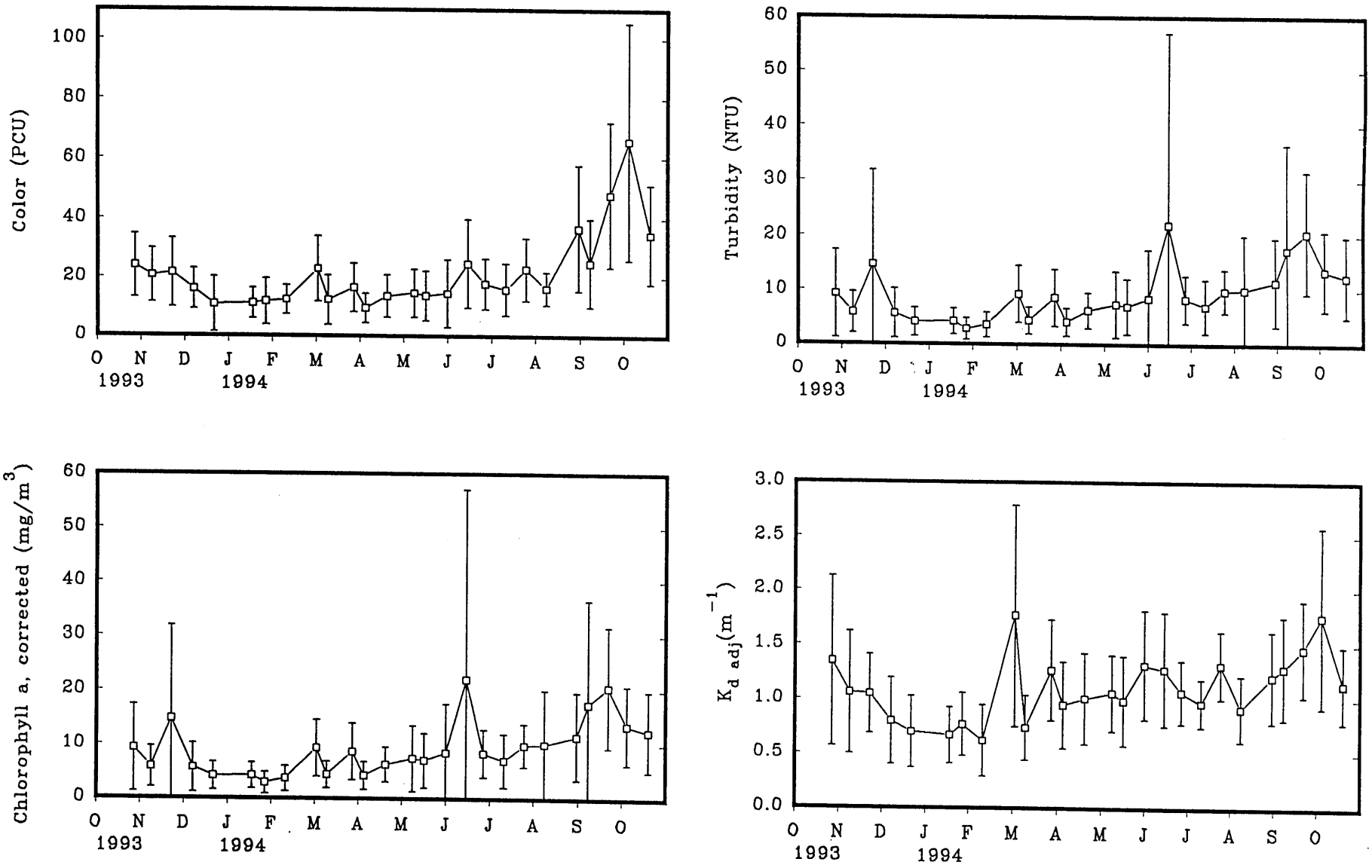

Figure 6. Seasonal patterns of water quality and clarity in Sarasota Bay.

Table 3. Mean and standard deviation of *in situ* water quality results in Sarasota Bay (n≈26 for each station). October 27, 1993, through October 19, 1994.

		Overall		Site 1		Site 2		Site 3		Site 4		Site 5		Site 6		Site 7	
		Mean	s.d.	Mean	s.d.	Mean	s.d.	Mean	s.d.	Mean	s.d.	Mean	s.d.	Mean	s.d.	Mean	s.d.
WATER QUALITY PARAMETERS																	
Turbidity	NTU	5.3	3.9	5.4	2.3	7.9	4.9	4.3	2.0	7.1	6.8	3.4	1.1	3.9	2.2	4.7	1.5
TSS	mg/l	12.8	7.0	12.3	4.7	17.0	10.6	11.1	4.1	15.5	10.7	10.3	4.1	12.4	3.7	10.8	3.2
VSS	mg/l	3.9	2.0	3.4	1.0	4.9	2.6	3.1	1.2	4.4	3.1	2.9	1.0	4.0	1.2	4.8	1.5
MSS	mg/l	8.9	5.4	8.9	4.0	12.0	8.1	8.0	3.2	11.1	7.7	7.5	3.5	8.3	3.0	6.0	2.3
Color	PCU	21	18	21	26	28	23	18	15	13	8	12	6	24	13	34	11
Conductivity	mmhos/cm	46.0	6.2	47.5	5.1	44.6	6.3	45.7	5.0	48.9	2.3	49.1	1.7	46.2	3.3	39.7	10.1
Salinity	ppt	29.9	4.4	30.9	3.7	28.9	4.4	29.6	3.6	31.9	1.7	32.1	1.3	30.0	2.4	25.4	7.0
Chl a (corr)	mg/m^3	9.2	10.7	4.9	4.4	8.9	6.2	5.9	3.4	6.1	3.4	4.7	2.5	12.2	7.9	22.3	20.6
Phaeo a	mg/m^3	2.8	3.3	1.5	1.4	3.1	2.8	2.0	2.1	2.1	2.2	1.1	0.9	3.9	2.7	6.2	5.6
Chl a	mg/m^3	11.3	12.3	6.0	5.2	11.1	7.9	7.4	4.6	7.6	4.6	5.6	3.0	15.0	8.9	26.7	23.0
Chl b	mg/m^3	0.5	2.1	0.1	0.0	0.1	0.2	0.1	0.0	0.1	0.0	0.1	0.0	0.1	0.2	2.9	4.9
Chl c	mg/m^3	2.3	2.1	1.5	1.0	2.3	1.6	1.6	0.8	1.8	0.8	1.3	0.6	3.1	1.7	4.4	4.0
FIELD ATTENUATION MEASUREMENTS																	
K_d(*in situ*), cosine	$m^{(-1)}$	1.24	0.59	1.15	0.67	1.53	0.54	1.13	0.40	1.07	0.66	0.83	0.19	1.17	0.39	1.82	0.53
K_d(*in situ*), scalar	$m^{(-1)}$	1.08	0.57	1.01	0.68	1.38	0.59	0.90	0.37	0.99	0.65	0.67	0.20	1.03	0.32	1.60	0.45
K_e	$m^{(-1)}$	1.29	0.60	1.27	0.68	1.57	0.55	1.16	0.42	1.15	0.66	0.86	0.22	1.20	0.39	1.87	0.53
Cosine photon zenith angle		0.56	0.09	0.49	0.09	0.51	0.06	0.57	0.09	0.53	0.08	0.58	0.07	0.63	0.10	0.61	0.09
Absorption coeff	$m^{(-1)}$	0.71	0.34	0.62	0.37	0.79	0.23	0.62	0.21	0.57	0.39	0.49	0.10	0.73	0.22	1.14	0.36
$K_{d\ adj}$	$m^{(-1)}$	1.11	0.53	0.97	0.58	1.33	0.50	1.02	0.39	0.98	0.62	0.76	0.20	1.09	0.38	1.64	0.47
LABORATORY ATTENUATION MEASUREMENTS																	
Raw, collimated	$m^{(-1)}$	2.23	0.82	2.08	0.63	2.80	0.86	1.95	0.56	2.22	1.15	1.61	0.30	2.14	0.56	2.85	0.53
Filtered, collimated	$m^{(-1)}$	0.43	0.22	0.51	0.41	0.47	0.27	0.40	0.13	0.33	0.06	0.35	0.05	0.43	0.13	0.53	0.15
Raw, diffuse	$m^{(-1)}$	1.87	0.64	1.85	0.48	2.34	0.72	1.65	0.44	1.86	0.93	1.41	0.22	1.72	0.37	2.26	0.46
Filtered, diffuse	$m^{(-1)}$	0.61	0.22	0.68	0.39	0.65	0.27	0.59	0.17	0.52	0.11	0.53	0.10	0.60	0.13	0.67	0.16

Attenuation coefficients determined with scalar (4pi) sensors generally were comparable to determinations with cosine sensors, although a linear regression ($n \approx 170$, $r = 0.8922$) of the two quantities (Figure 7), however, produced a slope of 0.924 and intercept of -0.05 implying that, for Sarasota Bay, the use of a scalar sensor to determine water column characteristics underestimates water column attenuation by nearly 8 percent on average.

Absorption coefficients calculated from field measurements generally represented a large fraction (58%) of the measured diffuse attenuation coefficient. The range in absorption contributions between stations was not large, with absorption contributing 52 percent to attenuation for Site 2 and 64 percent for Site 6.

A multiple linear regression of field-determined average cosine of the photon zenith angle included wind velocity, turbidity, and the cosine of the zenith angle in water (from sun elevations) as significant, but the model accounted for less than 20 percent of the variation in μ. The implication is that either additional field conditions such as waves or extent of clouds, or perhaps the varying spectra associated with time of day or varying cloud cover could exert important influences.

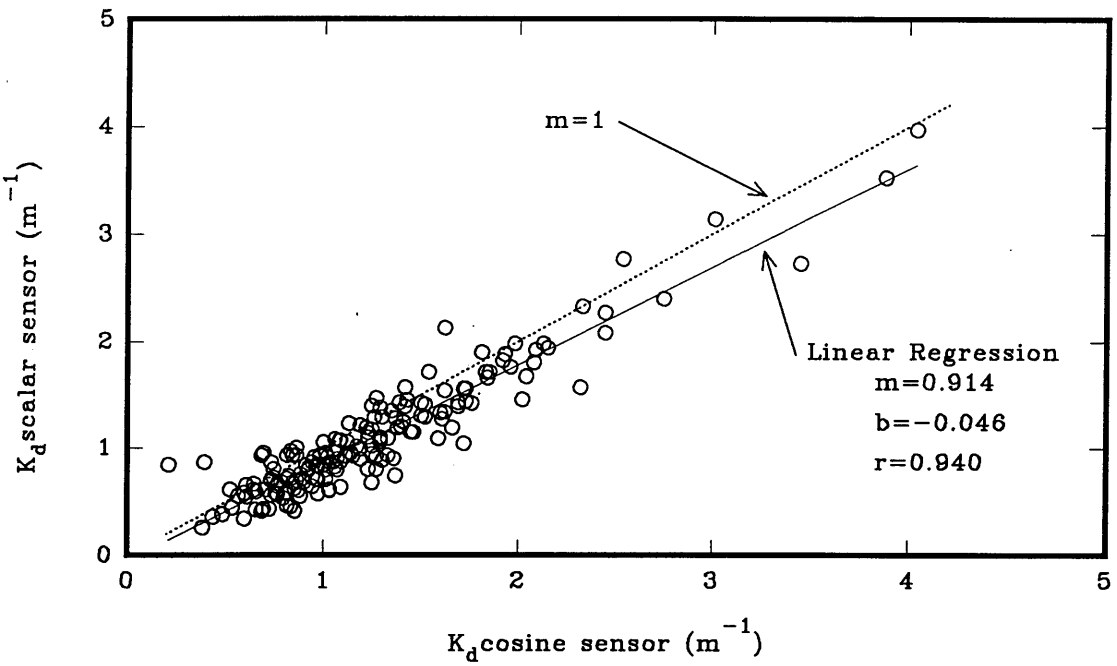

Figure 7. Comparisons of K_d determined with cosine and scalar sensors.

Adjusted Attenuation Coefficients

Both *in situ* and adjusted attenuation coefficients were extrapolated to provide an annual record of water column light attenuation. Daily values of the percentage of incident (subsurface) PAR were also calculated and averaged by site. Summary data are presented in Table 4 by station and indicate while the pathlength difference between Site 1 and Sites 5 or 6 is nearly 0.1 m, the difference in annualized light percentages between using unadjusted and adjusted K_d values are quite small and usually between 3 and 5 percent. Using unadjusted K_d values, the percent PAR remaining at the bottom of the water column ranges from 23 percent at Site 1, to 46 percent at Site 3, with all but Site 1 averaging near 42 percent. Light percentages calculated from $K_{d\ adj}$ were slightly higher, in keeping with an assumed zenith angle of zero.

Table 4. Annual station means of observed and adjusted K_d together with maximum depth of seagrasses and annualized water column light requirements as measured during midday hours. Calculated from extrapolated daily values. Percent PAR calculated as percent of incident (subsurface) irradiance.

Site	K_d (2pi) $m^{(-1)}$	Unadjusted PAR Light %	Solar* Elevation deg	Adjusted* Pathlength m	$K_{d\text{-}adj}$* $m^{(-1)}$	Maximum Depth m	PAR Light* Remaining %
1	1.09	23	45	1.19	0.92	1.63	28
2	1.45	45	49	1.16	1.26	0.58	50
3	1.05	46	55	1.12	0.95	0.79	49
4	0.97	42	58	1.10	0.89	0.99	45
5	0.89	35	62	1.09	0.75	1.33	38
6	1.13	44	62	1.09	1.04	0.77	47
7	1.81	42	59	1.11	1.63	0.50	45

* - calculated from individual data points

Although $K_{d\ adj}$ leads to a slight overestimate of the average percentage of light received at the maximum seagrass depths and makes a slight difference in annualized light regimes, it should be a more appropriate parameter to determine empirical relationships with water quality parameters, and to permit station comparisons. As a result, $K_{d\ adj}$ was included in the linear regression models described below.

Laboratory Attenuation Coefficients

The laboratory attenuation coefficients of field and lab blanks were used to determine a standard deviation among blanks of 0.03 m^{-1} and an approximate detection limit of 0.1 m^{-1} for laboratory measurements. Blanks averaged 0.241 m^{-1}, as calculation techniques were derived from literature beam attenuation coefficients (0.219 m^{-1}).

Comparison of the relative magnitudes of the four types of laboratory attenuation measurements reflect the underlying assumptions used to compute the attenuation coefficients. For both raw and filtered samples, attenuation of raw samples was greater than of filtered samples due to the presence of particulates. The attenuation coefficients of filtered samples represent attenuation attributable to water and to dissolved organic matter (color) and comprise between 20 percent and 30 percent of total attenuation.

For filtered samples, K_d computed with collimated light is less than the K_d for diffuse light, the result of the longer optical path length of diffuse light. For raw samples, however, attenuation of collimated light is greater than for diffuse light. This is the result of the calculation method for measurements with collimated light and of the assumption that the optical path length in the sample is equivalent to the path length in the blank. In reality, the path length of the raw sample can be much greater, and the resultant K_d is an overestimate, the degree of which is sample-specific and dependent on sample scattering.

Correlations of field and laboratory data indicate 30 percent to 35 percent of variation in field $K_{d\ adj}$ is unexplained by either $K_{dCOL\text{-}RAW}$ or $K_{dDIF\text{-}RAW}$ (Figure 8). Comparison of laboratory attenuation values to *in situ* measurements reveal that field values of K_d are not bracketed by $K_{dCOL\text{-}RAW}$ and $K_{dDIF\text{-}RAW}$ but are instead generally lower than either one. The discussion above has demonstrated that $K_{dCOL\text{-}RAW}$ may be an overestimate due to an underestimate of optical path length. The calculation method for diffuse laboratory attenuation can also produce an overestimate of K_d if path lengths are overestimated. Again any overestimate is sample specific. Spectral differences between sunlight and the laboratory light source may also contribute to the overestimate of laboratory attenuation, as quartz-halogen spectra are richer in the red wavelengths which are more rapidly absorbed by water. Attenuation coefficients for water, for example, are 0.219 m^{-1} with a quartz-halogen source, and 0.137 m^{-1} for sunlight. Chlorophyll, with it's distinct absorption peaks, should exhibit a similar dependence on incident spectral quality in determination of integrated absorption coefficients.

Regression Models of Attenuation

Multiple linear regressions were performed on attenuation coefficients as a function of the various water quality parameters, both for the study area as a whole and by station. Results for *in situ* measurements (both K_d (cosine sensor) and $K_{d\ adj}$) appear in Tables 5 and 6. Turbidity, followed by color and various chlorophylls were the most common

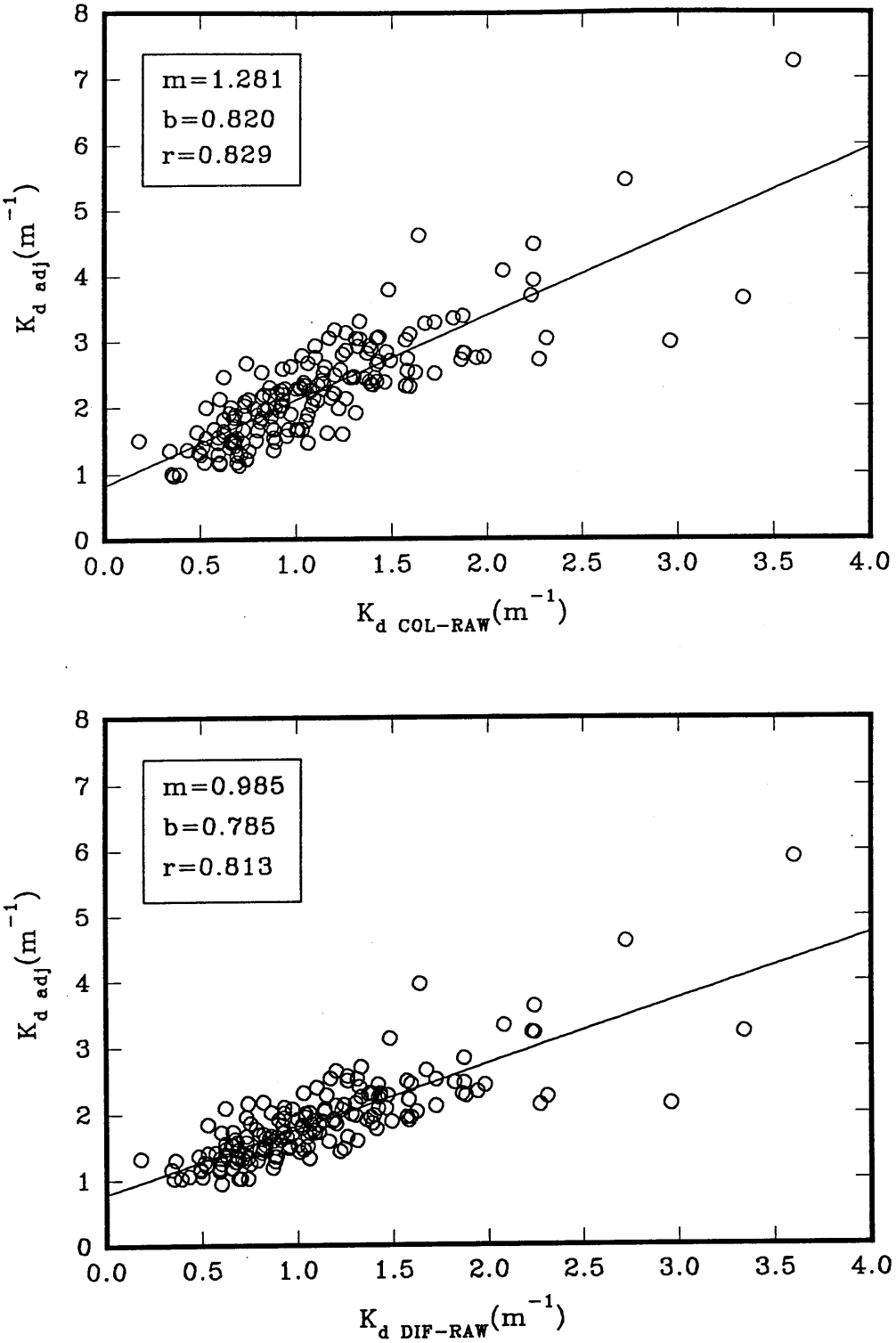

Figure 8. Agreement between field and laboratory attenuation coefficients.

Table 5. Overall and station-specific regression models of $K_{d\ (in\ situ,\ cosine\ sensor)}$ with water quality parameters.

K_d (*in situ*, cosine sensor)								
A/B* Independent Variables	**SITES**							
	Overall	**1**	**2**	**3**	**4**	**5**	**6**	**7**
Turbidity	0.1979/0.0691	0.0284/0.0509	0.4954/0.0782	0.1602/0.0884	0.3085/0.0741			0.4518/0.2263
TSS								
VSS								
MSS								
Color	0.3029/0.0205	0.2426/0.0186	0.4069/0.0148	0.0840/0.0144			0.1079/0.0136	
Cond								
Chl a corr					0.0335/0.0492			
Pheoa	0.0163/0.0263							
Chl a						0.4164/0.0412	0.1141/0.0206	
Chl b		0.0605/4.791						
Chl c				0.0169/0.1353				
Model r^2	0.7575	0.9399	0.8720	0.8582	0.8957	0.4164	0.7624	0.4518
Corrected r^2	0.7533	0.9317	0.8609	0.8379	0.8866	0.3920	0.7408	0.4269
Intercept	0.3538	0.1830	0.4956	0.2460	0.2363	0.5948	0.5304	0.7386
SE regression	0.29	0.18	0.21	0.16	0.23	0.15	0.20	0.41

* A = Contributing r^2
B = Partial regression coefficient

Table 6. Overall and station-specific regression models of $K_{d\ adj}$ with water quality parameters.

$K_{d\ adj}$								
A/B* Independent Variables	SITES							
	Overall	1	2	3	4	5	6	7
Turbidity	0.2085/0.0626	0.1448/0.0868		0.3744/0.0657	0.1268/0.0403	0.0882/0.0727	0.0618/0.0731	
TSS							0.1495/0.0418	
VSS			0.0301/0.0557				0.0824/0.1316	
MSS						0.0522/0.0328		
Color	0.2413/0.0170	0.0364/0.0170			0.5846/0.0424	0.0308/0.0145	0.3223/0.0154	0.6382/0.0163
Cond			0.1326/0.0462					
Chl a corr				0.1019/0.0602		0.2595/0.0793		
Pheoa								
Chl a	0.0280/0.0084	0.2025/0.0707	0.0352/0.0253					
Chl b			0.0492/0.1592			0.2449/0.3318	0.0511/0.0857	
Chl c		0.2080/0.4824						0.0454/0.0366
Model r^2	0.7505	0.7533	0.9231	0.9533	0.7652	0.8283	0.8148	0.7909
Corrected r^2	0.7462	0.7063	0.9060	0.9493	0.7448	0.7854	0.7685	0.7719
Intercept	0.3150	0.4268	2.537	0.2093	0.2201	0.7021	0.5192	0.5661
SE regression	0.27	0.31	0.10	0.17	0.18	0.20	0.16	

* A = Contributing r^2
B = Partial regression coefficient

parameters found significant, with color accounting for the larger portion of the variation of *in situ* attenuation for both K_d and $K_{d\ adj}$. The overall model accounted for over 75 percent of the variation of *in situ* K_d, with 95 percent confidence limits of the mean K_d equal to 1.24 m^{-1} $\pm$ 0.08 m^{-1} ($n \approx 178$). The individual station models typically had higher r^2 values than overall models, except at Site 5, the station with the lowest attenuation coefficient.

Intercept values for the models of *in situ* attenuation typically ranged between 0.18 and 0.59 m^{-1}, or roughly equivalent to the expected range in beam attenuation coefficients expected for water alone under optical path lengths ranging from 1.0 to 2.0. Site 7 was unusual with an intercept of 0.73 m^{-1}. The occasional negative regression coefficient emphasizes the fact that regression models are empirical relationships describing an existing set of data rather than a process-based description of the controlling light attenuation functions.

Overall, r^2 values for models of laboratory attenuation were generally much better than the similar models of *in situ* attenuation. Filtered samples (Tables 7 and 8) were regressed only against color and conductivity. The corrected r^2 of the overall model was 0.8099 ($n \approx 178$) with a 95 percent confidence interval of the mean $K_{dCOL\text{-}FILT}$ equal to 0.43 $\pm$ 0.05 m^{-1}. Intercepts for the models of filtered samples averaged 0.19 m^{-1} under collimated light, and 0.38 m^{-1} under diffuse conditions, or near the theoretical values of the beam attenuation of pure water under collimated and diffuse conditions. Sites 4 and 5, with comparatively low color values, displayed poorer fits of filtered attenuation against color. Site 7, with the lowest overall salinity, displayed an additional inverse correlation with salinity, implying a significant freshwater-associated dissolved (or less than 0.45 μm) component contributing to attenuation.

Regression of water quality parameters with the attenuation of raw samples also produced acceptable models (Tables 9 and 10) with color and turbidity accounting for roughly comparable amounts of variation in both $K_{dCOL\text{-}RAW}$ and $K_{dDIF\text{-}RAW}$. Smaller amounts of variation were linked with volatile suspended solids and chlorophyll *a*. The 95 percent confidence interval for $K_{dCOL\text{-}RAW}$ was 2.23 $\pm$ .08 m^{-1} and 1.87 $\pm$ 0.08 m^{-1} for $K_{dDIF\text{-}RAW}$. Better fits were obtained with individual station models for Sites 1-4.

Partitioning of Attenuation

The results of the partitioning of laboratory light attenuation are presented in Table 11 as K (m^{-1}) and as percentages of the total attenuation of raw samples in Table 12. Although the discussion above indicates that field and laboratory data may not be directly comparable, the assumptions used to compute laboratory attenuation are consistent for all measurements with diffuse light and for all measurements with collimated light and relative proportions of the partitioned components are useful to examine. Assumptions contained within the partitioning process which could alter the relative proportions are primarily those of optical path length, i.e., 1.0 for collimated light and 2.0 for diffuse

Table 7. Overall and station-specific regression models of $K_{d\ COL\text{-}FILT}$ with water quality parameters.

$K_{d\ COL\text{-}FILT}$								
A/B* Independent Variables	SITES							
	Overall	1	2	3	4	5	6	7
Color	0.8099/0.0112	0.9345/0.0153	0.9088/0.0110	0.8562/0.0082	0.3583/0.0043	0.4128/0.0046	0.7544/0.0088	0.0972/0.0061
Cond								0.2021/-0.0093
Model r^2	0.8099	0.9345	0.9088	0.8562	0.3582	0.4128	0.7544	0.9091
Corrected r^2	0.8088	0.9318	0.9050	0.8502	0.3315	0.3883	0.7447	0.9008
Intercept	0.1900	0.1820	0.1603	0.2463	0.2965	0.2710	0.2228	0.6915
SE regression	0.10	0.11	0.08	0.05	0.04	0.05	0.07	0.05

* A = Contributing r^2
B = Partial regression coefficient

Table 8. Overall and station-specific regression models of $K_{d\ DIF\text{-}FILT}$ with water quality parameters.

$K_{d\ DIF\text{-}FILT}$								
A/B* Independent Variables	SITES							
	Overall	1	2	3	4	5	6	7
Color	0.7288/0.0106	0.9373/0.0145	0.8522/0.0107	0.7764/0.0098			0.7108/0.0083	0.5529/0.0114
Cond					0.3689/-0.0290			
Model r^2	0.7288	0.9373	0.8522	0.7764	0.3689		0.7108	0.5528
Corrected r^2	0.7273	0.9347	0.8460	0.7670	0.3426		0.6987	0.5333
Intercept	0.3780	0.3747	0.3479	0.4136	1.9337		0.3997	0.2815
SE regression	0.12	0.10	0.11	0.08	0.09		0.07	0.11

* A = Contributing r^2
B = Partial regression coefficient

Table 9. Overall and station-specific regression models of $K_{d\ COL\text{-}RAW}$ with water quality parameters.

$K_{d\ COL\text{-}RAW}$								
A/B* Independent Variables	SITES							
	Overall	1	2	3	4	5	6	7
Turbidity	0.1041/0.1134	0.5800/0.2152	0.82261/0.1593	0.4027/0.1801	0.3193/0.1409	0.5030/0.2111		0.2752/0.0857
TSS								
MSS								
VSS	0.0168/0.0966							
Color	0.1004/0.0170	0.6314/0.0202	0.1379/0.0137					
Cond								
Chl a corr								
Chl a	0.0164/0.0112			0.3116/0.0703	0.0178/0.0487	0.0848/0.0311	0.1949/0.1188	
Chl b								
Chl c							0.0631/-0.3457	0.0857/0.0490
Model r^2	0.8915	0.9304	0.9381	0.9501	0.9689	0.8383	0.7716	0.8497
Corrected r^2	0.8891	0.9243	0.9328	0.9457	0.9662	0.8243	0.7517	0.8360
Intercept	0.7697	0.4919	1.1583	0.6500	0.8436	0.7246	1.4357	1.5738
SE regression	0.27	0.18	0.23	0.13	0.22	0.13	0.29	0.22

* A = Contributing r^2
B = Partial regression coefficient

Table 10. Overall and station-specific regression models of $K_{d\ DIF\text{-}RAW}$ with water quality parameters.

$K_{d\ DIF\text{-}RAW}$								
A/B* Independent Variables	SITES							
	Overall	1	2	3	4	5	6	7
Turbidity	0.1252/0.0977	0.4674/0.1481	0.1107/0.0991	0.3848/0.1477	0.0373/0.0796	0.4251/0.1418		0.4349/0.2060
TSS			0.0156/0.0173					
VSS	0.0123/0.0649						0.0623/0.0997	
MSS					0.0084/0.0283			
Color	0.1173/0.0144	0.7057/0.0163	0.1689/0.0129	0.0142/0.0064			0.0698/0.0107	0.1515/0.0175
Cond								
Chl a corr				0.0445/0.0514				
Chl a	0.0097/0.0067				0.0236/0.0466	0.01576/0.0309	0.0556/0.0167	
Chl b			0.0175/-0.6346					
Chl c								
Model r^2	0.9091	0.9088	0.9543	0.9513	0.9704	0.8747	0.8643	0.7867
Corrected r^2	0.9070	0.9009	0.9456	0.9446	0.9664	0.8636	0.8458	0.7673
Intercept	0.7160	0.7023	0.9601	0.5921	0.6274	0.7540	0.8110	0.6785
SE regression	0.20	0.15	0.17	0.11	0.17	0.08	0.15	0.23

* A = Contributing r^2
B = Partial regression coefficient

Table 11. Mean and standard deviation of partitioned laboratory attenuation coefficients presented as attenuation coefficients (see text). Units are $m^{(-1)}$. Attenuation due to non-chlorophyll suspended matter includes error terms plus the additional absorption produced by water, chlorophyll, color, and solids when optical path lengths are greater than 1.0.

		Collimated Light							Diffuse Light						
	(m^{-1})	Raw	Filtered	Particulate	Water	Color	Chl a	NCSM	Raw	Filtered	Particulate	Water	Color	Chl a	NCSM
Overall	mean	2.23	0.43	1.80	0.22	0.21	0.16	1.65	1.87	0.61	1.26	0.44	0.17	0.31	0.95
	s.d.	0.82	0.22	0.77		0.22	0.17	0.70	0.64	0.22	0.60		0.22	0.34	0.55
Site 1	mean	2.08	0.51	1.58	0.22	0.29	0.08	1.49	1.85	0.68	1.17	0.44	0.24	0.17	1
	s.d.	0.63	0.41	0.53		0.41	0.07	0.53	0.48	0.39	0.38		0.39	0.14	0.41
Site 2	mean	2.80	0.47	2.33	0.22	0.25	0.15	2.18	2.34	0.65	1.70	0.44	0.21	0.31	1.39
	s.d.	0.86	0.27	0.85		0.27	0.11	0.83	0.72	0.27	0.72		0.27	0.22	0.71
Site 3	mean	1.95	0.40	1.55	0.22	0.18	0.10	1.45	1.65	0.59	1.06	0.44	0.16	0.20	0.86
	s.d.	0.56	0.13	0.51		0.13	0.06	0.48	0.44	0.17	0.40		0.17	0.13	0.35
Site 4	mean	2.22	0.33	1.89	0.22	0.11	0.11	1.79	1.86	0.52	1.35	0.44	0.08	0.21	1.14
	s.d.	1.15	0.06	1.15		0.06	0.06	1.10	0.93	0.11	0.93		0.11	0.13	0.84
Site 5	mean	1.61	0.35	1.26	0.22	0.13	0.08	1.19	1.41	0.53	0.88	0.44	0.09	0.15	0.72
	s.d.	0.30	0.05	0.29		0.05	0.04	0.28	0.22	0.10	0.24		0.10	0.08	0.21
Site 6	mean	2.14	0.43	1.71	0.22	0.21	0.21	1.50	1.72	0.60	1.12	0.44	0.16	0.41	0.70
	s.d.	0.56	0.13	0.50		0.13	0.12	0.41	0.37	0.13	0.32		0.13	0.25	0.20
Site 7	mean	2.85	0.53	2.32	0.22	0.31	0.37	1.95	2.26	0.67	1.58	0.44	0.24	0.74	0.85
	s.d.	0.53	0.15	0.51		0.15	0.32	0.37	0.46	0.16	0.44		0.16	0.63	0.41

Table 12. Mean and standard deviation of partitioned laboratory attenuation coefficients presented as a percentage of the total laboratory attenuation (see text). Units are $m^{(-1)}$. Attenuation due to non-chlorophyll suspended matter includes error terms plus the additional absorption produced by water, chlorophyll, color, and solids when optical path lengths are greater than 1.0.

		Collimated Light							Diffuse Light						
	%	Raw	Filtered	Particulate	Water	Color	Chl a	NCSM	Raw	Filtered	Particulate	Water	Color	Chl a	NCSM
Overall	mean	100	20	80	11	9	6	73	100	34	66	26	8	15	51
	s.d.		8	8	4	7	5	9	0	10	10	7	9	12	15
Site 1	mean	100	24	76	12	12	4	72	100	37	63	25	11	9	55
	s.d.		12	12	4	13	3	14	0	13	13	6	14	7	17
Site 2	mean	100	17	83	8	9	5	77	100	29	71	20	9	13	58
	s.d.		8	8	2	8	4	10	0	10	10	5	10	9	16
Site 3	mean	100	21	79	12	9	5	74	100	37	63	29	9	12	51
	s.d.		6	6	4	5	2	6	0	9	9	8	7	5	11
Site 4	mean	100	17	83	11	5	5	79	100	31	69	27	4	11	58
	s.d.		5	5	3	3	2	5	0	10	10	8	6	4	11
Site 5	mean	100	22	78	14	8	5	73	100	39	61	32	7	11	51
	s.d.		4	4	2	3	2	5	0	10	10	5	8	5	10
Site 6	mean	100	21	79	11	10	9	70	100	36	64	27	9	23	42
	s.d.		6	6	4	4	4	6	0	6	6	6	6	10	10
Site 7	mean	100	19	81	8	11	12	69	100	30	70	20	10	30	39
	s.d.		6	6	1	5	7	9	0	8	8	4	8	18	18

light. Differing path lengths would alter the proportion of attenuation attributed to water and chlorophyll, and by difference, the remainder of the parameters.

For collimated light, attenuations due to water (11%), color (9%), and chlorophyll (6%) are roughly comparable, with the bulk of the attenuation (73%) attributed to non-chlorophyll suspended matter (NCSM). The non-linearity of partitioned attenuation with component is visible in the plot of K_{dCOLOR} as a function of color (Figure 9). (It should be recalled that the $K_{d\text{-}NCSM}$ contains all error terms as well.) For diffuse light, color, water, chlorophyll and NCSM contribute 8 percent, 15 percent, 26 percent, and 51 percent respectively. For individual stations, contributions mimic the water quality distributions. Sites high in color (Site 1 and 7) exhibited larger proportions due to color (12 percent and 11 percent, respectively) when compared to sites low in color (Site 4 and 5). Chlorophyll contributions range over a similar span, from 12 percent of total attenuation at Site 7, to 4 percent at Site 1. The partial attenuation of NCSM was high at all sites, and ranged between 69 percent and 79 percent, at Sites 7 and 4, respectively. Temporal variation in the proportions of contributing K values was typically less than 10 percent, although some stations (Site 7) and parameters (NCSM) were more variable under diffuse light conditions.

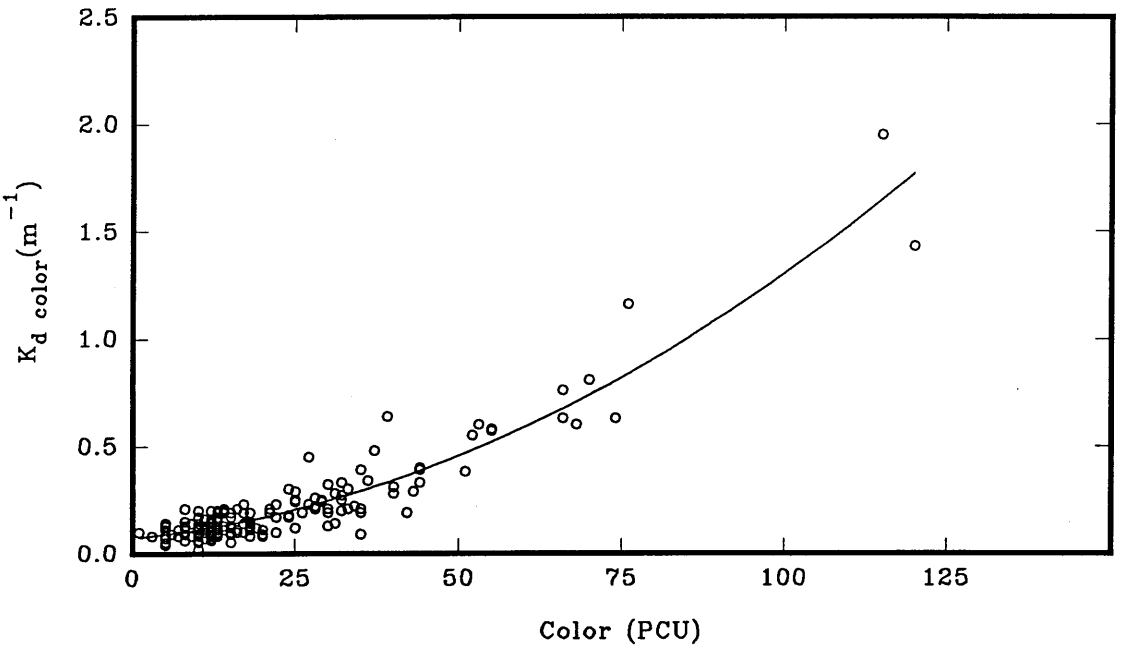

Figure 9. Relationship of measured color and partitioned attenuation attributed to color.

Spectral Absorption and Photosynthetically Usable Radiation

The absorption of photosynthetically usable radiation (PUR) is presented as a fraction of PUR lost to absorbing substances (other than water) in Table 13, calculated over a distance equivalent to the maximum depths of seagrasses recorded for the various stations (Table 1). Fractions of PUR lost to color, chlorophyll, and NCSM, computed as the ratios of the various absorption coefficients, are also presented as percentages of the total absorption. The fraction of absorption at Site 7 was higher on average than the remaining stations, 0.680 lost as compared to between 0.368 to 0.561 for the remaining stations. Proportions of absorption from color, chlorophyll and NCSM were generally consistent between stations, with color accounting for approximately 51 percent of absorption, and chlorophyll and NCSM accounting for 25 percent and 24 percent respectively.

The relative absorptions of PUR due to color, chlorophyll, and NCSM are substantially different from the partitioned K_d values (Table 14). When comparing the total and partitioned PUR fractions lost to the partitioned K_d values for reasonableness, the effects of scattering (included in the measurements of K), must be estimated and included in the measurements of PUR lost.

Fractions of PUR lost were determined using beam absorption coefficients and optical path lengths of 1.0 X seagrass maximum depths. If the assumption is made that *in situ* light in the water column rapidly becomes totally diffuse (path length = 2.0 X maximum depth) due to scattering, then absorption by color, chlorophyll, and NCSM should all increase two-fold. Since the optical path (and resultant additional absorption) has been increased by scattering due to the presence of suspended particulates, the increases in absorbance are assigned to the NCSM column and the percentages recalculated (Table 14). The partitioned PAR values for diffuse and collimated light as a percentage of total water column attenuation from Table 11 are also recalculated as a percentage of all non-water attenuation.

Adjustment of the PUR fractions for scattering and comparison with the partitioned K_d values (as percentages of attenuators other than water) exhibit comparable levels of attenuation attributable to NCSM, with chlorophyll and color absorption playing relatively minor roles. Additional differences between PUR fractions absorbed and partitioned attenuation can be attributed to spectral differences between the PUR and PAR determinations, together with the action spectra of the seagrasses themselves.

Epiphytic Attenuation

Epiphytic attenuation was determined on eleven occasions at Site 1 through 6 over the course of the year, but was not possible at Site 7 due to the die-back of seagrasses at that station. Mean and standard deviations of attenuation (as percent) appear in Table 15 and illustrate that while considerable variation exists, epiphytic cover in Sarasota Bay reduces

Table 13. Fraction of maximum PUR absorbed by water column components (influence of scattering not included). Components proportional to parameter absorption coefficients. Presented as fraction and as a percent of the total fraction. Computed for the maximum depth limits reported in Table 1.

		Fraction PUR Lost				Percentage of Total PUR Lost			
		Total	Color	Chl a	NCSM	Total	Color	Chl a	NCSM
Overall	Mean	.497	.259	.125	.112	100	51	25	24
	s.d.	.166	.137	.062	.063		14	8	12
Site 1	Mean	.462	.281	.087	.092	100	55	21	24
	s.d.	.197	.206	.035	.035		16	8	12
Site 2	Mean	.559	.295	.117	.147	100	51	21	27
	s.d.	.135	.135	.031	.075		13	4	12
Site 3	Mean	.446	.245	.094	.106	100	53	22	25
	s.d.	.160	.142	.030	.056		15	5	14
Site 4	Mean	.405	.158	.120	.126	100	40	31	29
	s.d.	.116	.064	.023	.110		13	6	15
Site 5	Mean	.368	.206	.082	.079	100	55	22	22
	s.d.	.054	.061	.019	.031		12	5	9
Site 6	Mean	.561	.292	.165	.104	100	51	29	20
	s.d.	.117	.118	.061	.027		10	8	7
Site 7	Mean	.680	.340	.207	.131	100	50	30	20
	s.d.	.094	.084	.081	.026		10	9	5

Table 14. Partitioned laboratory attenuation presented as the percentages of non-water attenuation for collimated and diffuse light, compared with the percentage contributions of PUR absorption, adjusted for scattering effects.

		Partitioned PAR attenuation as % of non-water attenuators						PUR Lost as a % of Total ---Adjusted for Scattering---		
		-------- Collimated ---------			---------- Diffuse ----------					
		Color	Chl a	NCSM	Color	Chl a	NCSM	Color	Chl a	NCSM
Overall	Mean	10	7	82	10	21	69	25	13	62
	s.d.	8	6	11	12	15	22	7	4	6
Site 1	Mean	13	5	82	14	13	73	28	10	62
	s.d.	14	4	17	18	11	27	8	4	6
Site 2	Mean	9	7	84	11	18	71	26	11	64
	s.d.	7	5	12	10	14	23	6	2	6
Site 3	Mean	9	6	85	10	16	74	26	11	63
	s.d.	5	2	7	10	7	16	8	3	7
Site 4	Mean	5	5	90	5	15	80	20	15	64
	s.d.	3	1	3	9	3	10	6	3	7
Site 5	Mean	11	5	84	8	16	77	28	11	61
	s.d.	4	2	6	11	7	15	6	3	5
Site 6	Mean	10	10	80	11	30	58	25	15	60
	s.d.	6	2	8	9	6	12	5	4	4
Site 7	Mean	13	14	73	10	41	48	25	15	60
	s.d.	6	9	11	12	22	28	5	4	3

Table 15. Seasonal and station means of % attenuation of PAR due to epiphytic material in Sarasota Bay ($n \approx 5$ for each station-date).

	Overall		Site 1		Site 2		Site 3		Site 4		Site 5		Site 6	
DATE	Mean	s.d.	Mean	s.d.	Mean	s.d.	Mean	s.d.	Mean	s.d.	Mean	s.d.	Mean	s.d.
12/ 6/93	57.6	11.6	61.2	10.1	62.2	10.3	64.3	6.6	62.3	8.0	38.3	5.7	57.3	7.9
1/11/94	71.1	26.2	98.9	1.1	95.9	1.2	43.5	21.4	89.1	6.1	46.2	16.3	52.8	9.6
2/28/94	40.5	15.2	53.2	13.5	32.3	9.7	28.7	7.2	33.8	13.2	41.0	16.4	53.8	15.2
3/21/94	53.7	14.1	43.3	12.2	53.6	13.3	67.8	6.6	65.6	9.9	47.0	6.9	44.9	16.3
4/19/94	40.1	16.3	36.1	4.9	41.2	13.0	50.5	8.2	30.7	5.5	29.4	14.5	52.5	29.7
5/16/94	42.2	13.2	38.1	6.8	25.8	7.0	61.0	9.0	39.9	3.6	50.9	11.6	37.3	6.6
6/14/94	32.1	12.9	48.4	5.8	22.9	7.7	35.9	4.7	19.0	5.0	21.9	6.9	44.4	8.8
7/12/94	42.3	10.9	35.1	4.4	39.7	15.2	57.0	8.5	41.2	7.1	36.2	5.1	44.5	10.0
8/22/94	38.0	18.3	30.3	3.5	61.0	1.7	63.0	4.1	17.7	1.7	20.1	5.2	36.2	4.5
9/19/94	64.7	16.5	72.2	8.3	89.7	2.4	63.0	4.3	70.1	6.3	45.0	11.5	48.1	8.1
10/21/94	63.5	26.3	54.9	12.1	91.0	6.8	73.6	4.5	13.1	11.0	67.5	7.8	80.6	8.2
YEAR	49.6	21.2	52.0	20.5	55.9	26.7	55.3	15.6	43.9	24.6	40.3	16.1	50.2	16.5

available light by nearly 50 percent as a yearly average, and ranges from 13 percent to 98 percent at various stations over the year. Annual averages of epiphytic attenuation varied less between stations, from a low of 40 percent at Site 5, to 56 percent at Site 2. Seasonal variations were similar among stations with higher epiphyte attenuations observed during the colder months when blade growth rates and turnover are low (Figure 10). Lowest epiphytic densities were observed between April and August coinciding with reported periods of maximum seagrass production (Tomasko *et al.*, In review).

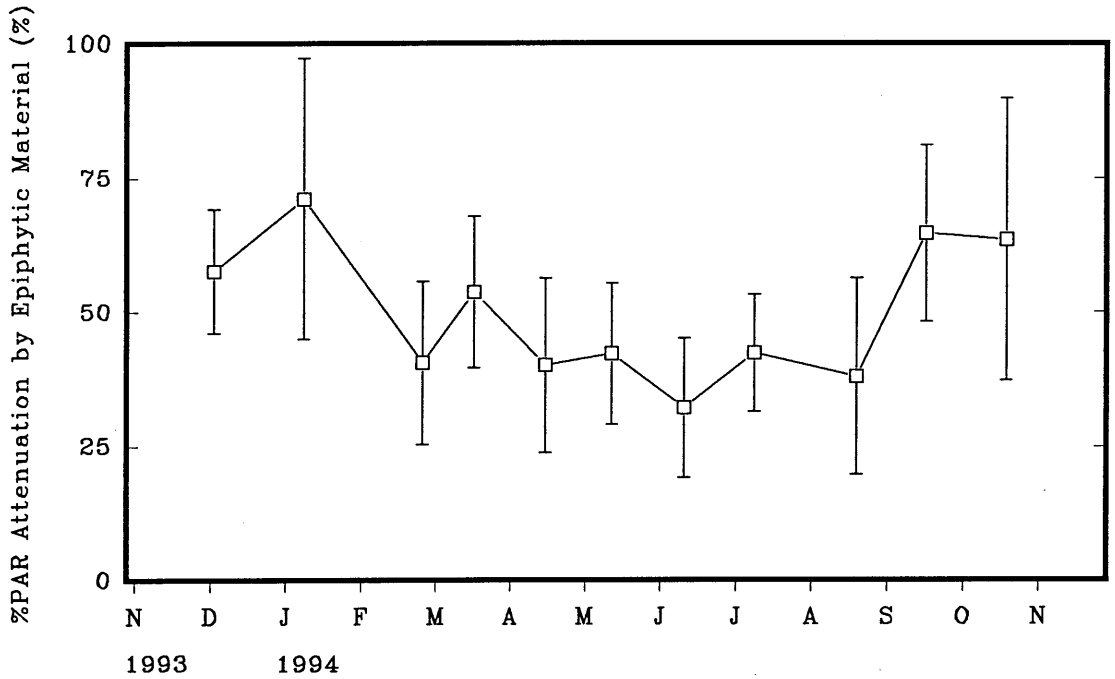

Figure 10. Seasonal variations in PAR attenuations due to epiphytic material on seagrass blades in Sarasota Bay.

When considering the extent to which epiphytic cover shades seagrasses the technique used should be reviewed. Noteworthy is the fact that the necrotic tissues (and any associated epiphytes) were **removed** prior to the determination of attenuation. Particularly for *Halodule*, the upper necrotic portion of the blades supported the densest epiphytic cover. In beds with reasonably high shoot densities, the upper necrotic/epiphytic zone would provide **additional** attenuation not measured by the procedure used.

Light Available to the Seagrasses

The combination of epiphytic **and** water column attenuation was used to compute the percentage of PAR available in the water column at maximum depth limits (Table 16)

Table 16. Monthly averages of the percent of PAR remaining in the water column at maximum seagrass depths. Computed from extrapolated annualized K_{adj} and epiphytic attenuation.

	Site	Oct	Nov	Dec	Jan	Feb	Mar	Apr	May	Jun	Jul	Aug	Sep	May-Sep	Year
Water Column PAR	1*	7	20	36	38	41	39	25	34	32	30	32	12	28	28
	2*	34	46	56	61	59	40	43	58	44	55	53	47	51	50
	3^	30	55	71	68	57	55	50	45	35	43	47	36	41	49
	4*	41	46	55	56	74	43	38	38	27	37	49	39	38	45
	5^	34	35	40	46	61	46	39	38	36	30	25	31	32	38
	6^	33	48	56	63	60	57	58	50	39	37	34	30	38	47
	7	46	35	48	50	56	54	51	41	36	49	40	40	41	45
All Stations															
Minimum		7	20	36	38	41	39	25	34	27	30	25	12	26	28
Maximum		46	55	71	68	74	57	58	58	44	55	53	47	51	50
Average		32	41	52	55	58	48	43	43	36	40	40	34	39	43
Halodule															
Minimum		7	20	36	38	41	39	25	34	27	30	32	12	27	28
Maximum		46	46	56	61	74	54	51	58	44	55	53	47	51	50
Average		32	37	49	51	58	44	39	43	35	43	43	35	40	42
Thalassia															
Minimum		30	35	40	46	57	46	39	38	35	30	25	30	31	38
Maximum		34	55	71	68	61	57	58	50	39	43	47	36	43	49
Average		33	46	55	59	59	53	49	44	37	37	35	32	37	45

* *Halodule*
^ *Thalassia*

and the PAR available to the photosynthetic portions of seagrass blades (Table 17). To permit station intercomparisons, $K_{d\ adj}$ was used to compute light levels at maximum depths. Averaged over a year, the values should approximate the annualized light requirements of the various seagrass species. The **plant-available** light so determined **cannot** be used as a management goal for **water column** clarity alone unless epiphytic growth and attenuation are non-existent.

As the annualized average light requirements are produced from the extrapolation of a single midday measurement of attenuation to subsequent days, estimates will be improved with increasing density of data. Estimates may be low if an inordinate number of high turbidity conditions are sampled, or may be high if measurements are only collected during quiescent conditions. The 26 samplings for this study sampled two highly turbid conditions related to storm events, which were extrapolated to roughly 28 days. The wet season was delayed in the onset from normal historical conditions, with color likely lower than long term averages, but heavy rains during the latter portion of the study may have offset the initial low color values. The annualized light requirement (as a percentage) cannot be used to determine the total energy requirement of the seagrasses (in $\mu E/cm^2/year$) as data from periods other than midday (when attenuation is higher) were not collected.

Except for Site 1, between 38 and 50 percent of incident irradiance (just below the surface) was available at the bottom of the water column. At Site 1, 28 percent of the subsurface irradiance was available as an annual average. Epiphytic attenuation reduced PAR approximately an additional 50 percent, such that the amount received by the photosynthetic portion of the seagrass blades averaged between 21 percent to 24 percent during midday hours for most stations. Site 1, with *Halodule* present, was anomalous in that annual water column light availability was 28 percent of incident, and that received by the seagrasses was 12 percent as an annual average. Other stations with *Halodule* both averaged 21 percent, while *Thalassia* sites averaged 22 percent, 23 percent, and 24 percent over the year.

Presentation of water column and plant-available PAR on a monthly basis reveals, however, some noteworthy agreements both among species and during certain periods of the year. Figure 11 illustrates the monthly average PAR available to the plant at the maximum seagrass depths. (Extrapolated and annualized $K_{d\ adj}$ was used for all calculations.)

The sites where *Halodule* was present (Sites 1, 2,and 4) exhibited the most variation throughout the year, with minima of less than 10 percent during February. As minima coincided with maximum water clarity, epiphytic attenuation is responsible for the low levels of light available to the plant. As previously mentioned, the heaviest epiphyte coverages were coincident with periods of minimum productivity, blade elongation, and turnover. During the periods of May through September (during periods of peak

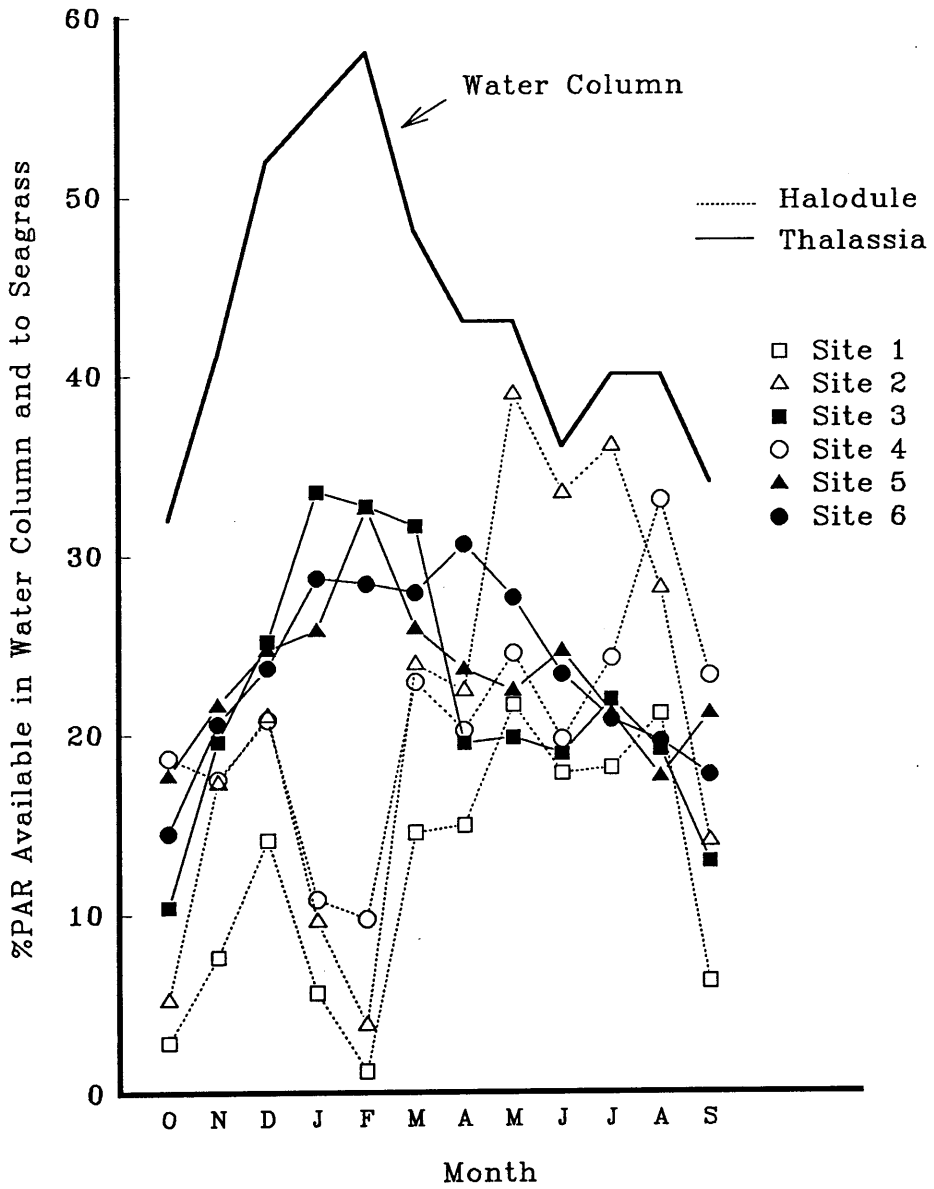

Figure 11. Monthly averages of PAR available to the seagrass blades after water column and epiphyte attenuation, as a percent of incident during midday hours.

Table 17. Monthly averages of the percent of PAR available to the seagrass blades after water column and epiphytic attenuation at maximum seagrass depths. Computed from extrapolated annualized K_{adj} and epiphytic attenuation.

	Site	Oct	Nov	Dec	Jan	Feb	Mar	Apr	May	Jun	Jul	Aug	Sep	May-Sep	Year
Plant															
Available PAR	1*	3	8	14	6	1	15	15	22	18	18	21	6	17	12
	2*	5	17	21	10	4	24	22	39	33	36	28	14	30	21
	3^	10	20	25	34	33	32	20	20	19	22	19	13	19	22
	4*	19	18	21	11	10	23	20	25	20	24	33	23	25	21
	5^	18	22	25	26	33	26	24	22	25	21	18	21	21	23
	6^	15	21	24	29	28	28	31	28	23	21	20	18	22	24
	7	-	-	-	-	-	-	-	-	-	-	-	-		-
All Stations															
Minimum		3	8	14	6	1	15	15	20	18	18	18	6	17	12
Maximum		19	22	25	34	33	32	31	39	33	36	33	23	30	24
Average		12	17	22	19	18	24	22	26	23	24	23	16	22	21
Halodule															
Minimum		3	8	14	6	1	15	15	22	18	18	21	6	17	12
Maximum		19	18	21	11	10	24	22	39	30	36	33	23	33	21
Average		9	14	19	9	5	20	19	28	24	26	27	14	24	18
Thalassia															
Minimum		10	20	24	26	28	26	20	20	19	21	18	13	19	22
Maximum		18	22	25	34	33	32	31	28	25	22	20	21	22	24
Average		14	21	25	29	31	28	25	23	22	21	19	17	21	23

* *Halodule*
^ *Thalassia*

growth), however, plants at all *Halodule* sites received between 17 percent and 30 percent of incident PAR, averaging 24 percent.

Sites where *Thalassia* was present exhibited very similar PAR levels at the plant surface during the growing season. Between May and September at all *Thalassia* stations, PAR after epiphytic attenuation ranged between 19 percent and 22 percent. Light levels during the remainder of the year were much higher than experienced at the *Halodule* sites, reaching maxima of near 30 percent during late winter and early spring.

Halodule appears to be able to tolerate at least short periods of extremely low light levels, and PAR received by the plant during winter can average well below 20 percent. *Thalassia*, on the other hand, was present in areas which, when water column attenuation was coupled with epiphytic coverages, experienced more modulated and higher light levels throughout the year. Both species received similar levels of total PAR, or near 20 percent of incident, during the period of peak growth.

Depth Limits of Seagrasses

Attenuation coefficients and maximum depth limits of seagrasses at the various sites were compared to determine if clarity could be used to predict depth limits. (Data from Site 7 were not included due to the disappearance of grasses at this site.) Correlations between site-specific study means of attenuation coefficients ($K_{d\ adj}$) and maximum depths are suggestive (Figure 12a), but are not significant ($P<0.20$), and indicate that other factors may contribute to seagrass depth limitations. Removal of Site 1 data as an outlier improves the relationship substantially (Figure 12b) to where $P>0.05$. Using all sites and $K_{d\ adj}$ improved the relationship slightly to where $P\approx 0.1$.

Due to the apparent seasonality of light regimes in Sarasota Bay and to the substantial attenuation provided by epiphytes, extrapolated daily water column attenuation coefficients at maximum seagrass depths (z_{max}) were increased for the site and season-specific epiphytic percent attenuation (EpiAttn) by:

$$K_{d\ total} = \frac{-\ln\left((1- EpiAttn/100) \bullet e^{-K_{d\ adj} \bullet z_{max}} \right)}{z_{max}}$$

and averaged over the May to September period. The regression of maximum depth as a function of the adjusted $K_{d\ total}$ (Figure 13) is very good ($r=0.9225$, $P>0.01$) and includes all six stations. The regression without Site 1 data is again better than when all sites are considered. To account for the differences in this site, the effectiveness of the adjustment for solar elevation (which ignores scattering effects) may be responsible, and as a result, relationships determined with data collected nearer solar noon should be more reliable. Physical differences noted at the site include higher current regimes than

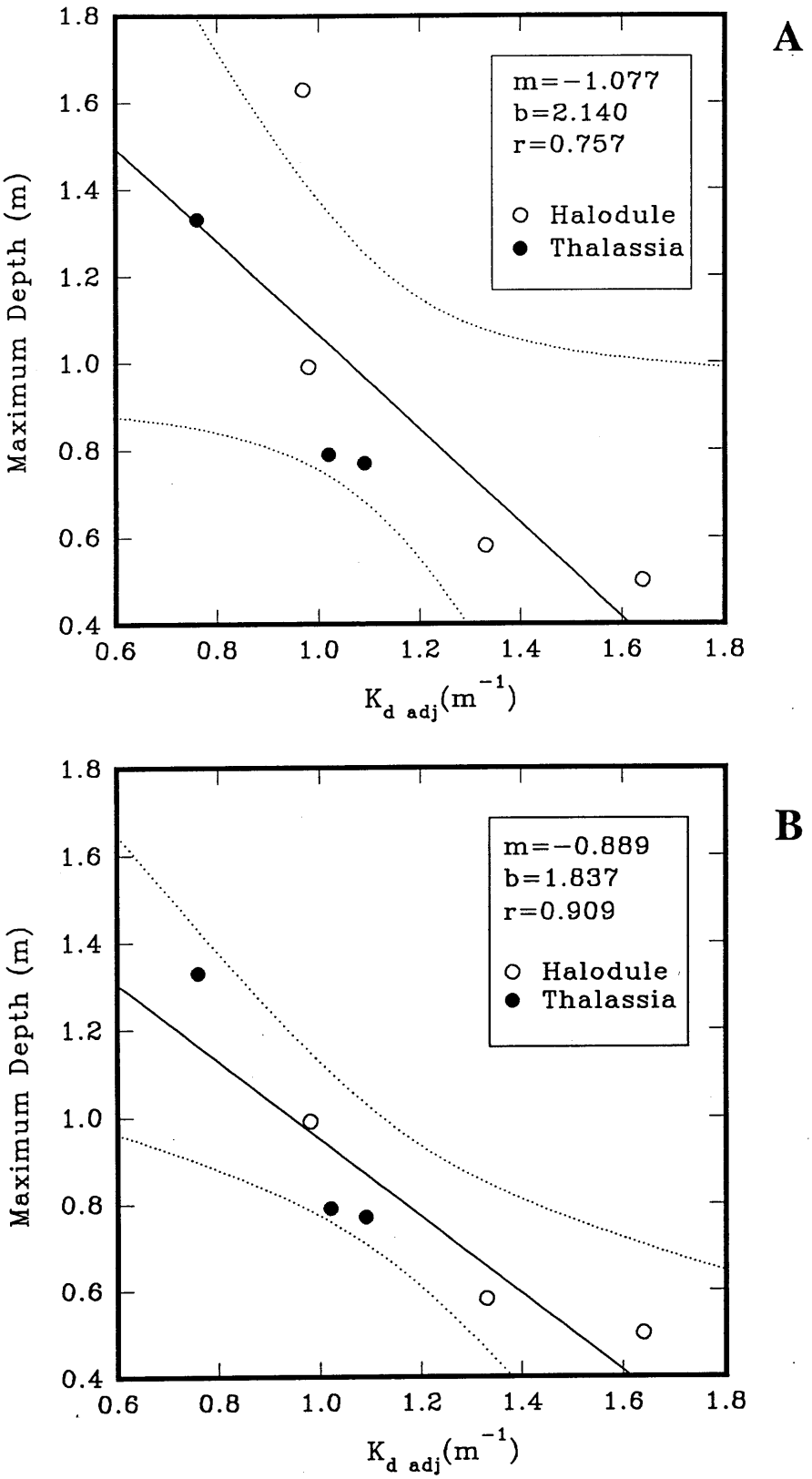

Figure 12a. Maximum depths of seagrasses as a function of mean $K_{d\ adj}$, all stations included. Dotted lines are the 95% confidence interval of the regression.

Figure 12b. Maximum depths of seagrasses as a function of mean $K_{d\ adj}$, Site 1 data omitted. Dotted lines are the 95% confidence interval of the regression.

observed at other locations. The site, however, does not appear to be current-limited as attenuation coefficients would be expected to be less than observed for the remaining deep edges. It is possible that the higher currents at Site 1 are more effective in removing the necrotic portion of the blades and the associated epiphytes, such that *in situ* attenuations due to epiphytes are more closely represented by the method used for laboratory determinations.

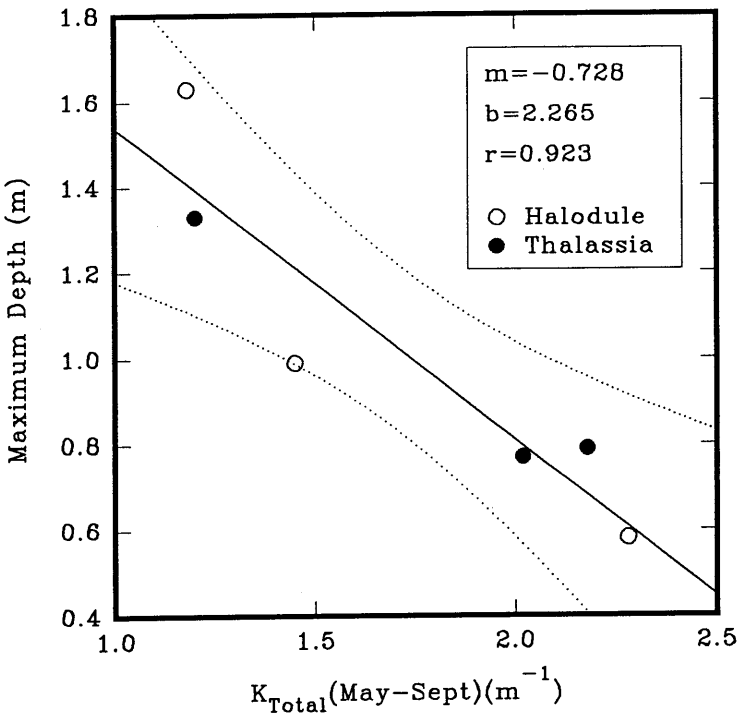

Figure 13. Maximum depth of seagrasses as a function of K_{TOTAL} (May-Sept), the total attenuation due to water column and epiphytes during the growing season.

SUMMARY

A data intensive study collected biweekly *in situ* measurements of water column attenuation, related water quality parameters, and remeasured attenuation under a variety of controlled conditions in the laboratory. (*In situ* data were collected between 1000 and 1400 hours, local time, and so averaged or annualized attenuation coefficients or light levels refer only to conditions near solar noon and cannot be used to compute total incident irradiance (μE/yr) required by the seagrasses.) A lower frequency (approximately monthly) of epiphytic attenuation and spectral absorption determinations were also conducted. Water column attenuation was partitioned into the fractions

contributed by the water itself, color, chlorophyll, and non-chlorophyll suspended matter, and empirical regression models developed for field and laboratory attenuation as a function of the water quality parameters measured (turbidity, solids, color, and chlorophylls).

The average PAR remaining in the water column at the maximum depth extent of two species of seagrasses (*Thalassia* and *Halodule*) ranged between 23 percent and 46 percent, averaging 40 percent. A consistent sampling bias, however, indicated that the 23 percent (Site 1) was certainly an underestimate, as these data were collected when solar angles were the farthest from solar noon. Average annual PAR at the maximum depths ranged between 35 percent and 46 percent (averaging 42%) in the absence of Site 1 data. Comparisons of average annual attenuation coefficients with maximum depths of grasses were suggestive, but not significant as long as data from all sites (including the site collected furthest from solar noon) were included.

Seasonal patterns of water column attenuation reflected the composite effects of patterns of turbidity or solids, chlorophyll, and color. Attenuation coefficients were low during the winter when biological activity and freshwater inflow was low, except during storm events when turbidity and solids were increased due to wind and wave action. As chlorophyll levels increased in summer and early fall, attenuation coefficients also increased. The onset of the wet season, and subsequent higher color values also coincided with increases in K_d.

Different stations were affected to differing degrees by various attenuators, with Sites 1 and 7 heavily influenced by color, and other sites more influenced by turbidity or solids. Overall sites, regression models of $K_{d\ adj}$ (K_d adjusted for solar elevation angle) indicated that color, turbidity, and chlorophyll *a* accounted for nearly 86 percent of the variation in attenuation, with most of the attenuation produced by color.

Laboratory partitioning of attenuation, however, in which the attenuation due to color (and water) was measured directly, indicated that most attenuation was attributed to the absorption and scattering of PAR by non-chlorophyll suspended matter. Investigations of the spectral absorption of various attenuating components supported the dominance of non-chlorophyll suspended matter, once estimates of scattering and the resultant additional absorption due to a longer optical path length was added to the measured absorptions. Overall stations, non-chlorophyll suspended matter accounted for between 60 and 70 percent of attenuation.

Epiphytic attenuation was measured by scraping the material from the productive seagrass blades, measuring PAR transmission through the suspension, and correcting for any difference between blade area scraped and suspension area measured. Epiphytic attenuation averaged 50 percent for the study as a whole, with individual station-date averages ranging between 13 percent and 98 percent. Epiphytic attenuation was much higher in the winter when blade turnover is low.

Levels of PAR available to the seagrass blade were computed from $K_{d\ adj}$ and epiphytic attenuation combined, and averaged 21 percent on an annual basis with all stations combined. (The levels of PAR available to the plant cannot be used as management goals for water column clarity unless epiphytic attenuation is zero.) Annual averages of PAR received by the seagrasses at individual sites ranges from 12 percent to 24 percent, with Site 1 an apparent outlier, as remaining stations range between 21 and 24 percent.

Interesting seasonal patterns of PAR received by the plants emerged by species. *Thalassia* received the highest levels of light in the year during the winter months. *Halodule* was apparently able to tolerate extremely low levels of PAR during the winter, often below 10 percent. Both species, however, received an average of near 20 percent (after **combined** attenuation of water column and epiphytes) during the growing season (May through September). Calculation of total attenuation (water column and epiphytic attenuation combined) and comparison with seagrass depth limits produced significant regressions even with all station data.

The use of empirical regression models for the direction of management efforts should be performed with caution, as the regressions are not necessarily functional relationships. This is demonstrated when comparing regression results (in which color appeared dominant) with the summary values of partitioned attenuation (in which non-chlorophyll suspended matter accounted for a larger proportion of water column attenuation. More weight should be placed on the partitioned results, in that they reflect measurements of partitioned components, and are supported as well by the results of the spectral absorption work.

The relative magnitude of epiphytic attenuation also complicates management decisions. Nutrient control for chlorophyll reduction will not directly improve water column clarity substantially. The control of nutrients, however, may reduce epiphytic attenuation, which could extend seagrass maximum depths. Conversely, control of solids and resultant improvement in water column clarity may allow additional epiphytic growth, as epiphytes are typically denser with increasing light levels (decreasing depths). If extension of maximum depths for seagrasses is desired, however, the uncertainty of epiphyte response to changing nutrient loadings would urge that epiphyte attenuation be included in any monitoring program.

REFERENCES

Baker, K.S. and R.C. Smith. 1982. Bio-optical classification and model of natural waters. 2. Limnol. Oceanogr. 27(3):500-509.

Butler, W. 1962. Absorption of light by turbid materials. J. Opt. Soc. Am. 52:292-299.